Analysis of the streamflow extremes and long term water balance in Liguria Region of Italy using a cloud permitting grid spacing reanalysis dataset

Francesco Silvestro[1],Antonio Parodi[1], Lorenzo Campo[1] , Luca Ferraris[1]

[1]{CIMA Research Foundation, Savona, Italy}

Correspondence to: francesco.silvestro@cimafoundation.org

Abstract

Characterizing the hydrometeorological extremes, in terms of both rainfall and streamflow, as well as the estimation of long-term water balance indicators are essential issues for flood alert and water management services. In recent years, simulations carried out with meteorological models are getting available at increasing spatial and temporal resolutions (both historical reanalysis and near real-time hindcast studies): thus, these meteorological datasets can be used as input for distributed hydrological models to drive long-period hydrological reanalysis. In this work we adopted a high resolution (4 km-spaced grid, 3-hourly) meteorological reanalysis dataset that covers Europe as a whole for the period between 1979 and 2008. This reanalysis dataset was used together with a rainfall downscaling algorithm and a rainfall bias correction technique in order to feed a continuous and distributed hydrological model. The resulting modelling chain allowed to produce long time series of distributed hydrological variables, inter alia streamflows and evapotranspiration for Liguria (N-W Italy), and the western Mediterranean areas that have been most impacted by severe hydro-meteorological events.

The available raingauges were compared with the rainfall estimated by the dataset, and then used to perform a bias correction in order to match the observed climatology. An analysis of the annual maxima discharges derived by simulated streamflow time series was carried out by comparing the latter with the observations (where available) or a regional statistical analysis

1 (elsewhere). Eventually, an investigation of long-term water balance was performed by

2 comparing simulated runoff ratios with the available observations.

3 The study highlights the limits and the potentialities of the considered methodological

4 approach in order to undertake an hydrological analysis in study areas mainly featured by

5 small basins, thus allowing to overcome the limits of observations which are punctual and in

6 some cases not fully reliable.

1   Introduction

8 The estimation of the magnitude and the probability of occurrence of a certain streamflow is

9 an important task for a number of purposes: risk assessment, design of structural protections

10 against flooding, civil protection, and early warning.

11 The standard approach based on the use of streamflow observations to carry out a statistical

12 analysis on a specific outlet (Kottegoda and Rosso, 1997) is not always possible because of

13 the lack of measurements: this problem can be tackled by means of a frequency

14 regionalization approach (De Michele and Rosso, 2002) exploiting both observed and

15 modelled streamflow (Boni et al., 2007).

16 On the other hand, studies and methodologies regarding the management of water resources

17 and drought also have an important role, especially in the perspective of possible future

18 changes in climate and water needs (Calanca et al., 2006; Fu et al., 2007; Döll and Müller,

19 2012; Asadieh and Krakauer, 2017). In this case, the analysis of long-term water balance

20 components is of primary importance and the evaluation of total runoff and

21 evapotranspiration becomes crucial.

22 In the last decades, the use of meteorological reanalyses to study basins behaviour in different

23 hydrological regimes has become quite frequent, due to the increased reliability and space-

24 time resolution of NWP models. Among many others, Choi et al. (2008) investigated the

25 feasibility of temperature and precipitation data of the North American Regional Reanalysis

(NARR, about 32 km grid spacing) for hydrological modelling in northern Manitoba watersheds, while Bastola and Misra (2013) showed that reanalysis products outperformed other four meteorological datasets, when used as a large-scale precipitation proxy for hydrological response simulations.

Furthermore, Krog et al. (2015) used ECMWF interim reanalysis (ERA-Interim, about 70 km grid spacing) as input to model the hydrological response of one of the largest rivers in Patagonia; similarly, Nkiaka et al. (2017) investigated the potential of using global reanalysis datasets in the data-scarce Sudan-Sahel region.

The CORDEX (COordinated Regional climate Downscaling Experiment, Giorgi et al. 2009) initiative is aiming at producing regional climate change projections worldwide to be fed into impact, adaptation and disaster risk reduction studies using fine-scaled regional climate models (RCM) forced by different GCMs of the CMIP5 (Coupled Model Intercomparison Project Phase 5, CMIP5) archive. Along these lines, Kotlarski et al. (2014) confirmed, with simulations on grid-resolutions up to about 12 km (0.11°), the capability of RCMs to correctly reproduce the main features of the European climate for the period 1979-2008. However they also exhibit relevant modeling errors concerning some metrics, certain regions and seasons: as an example, precipitation biases are in the ±40% range while seasonally and regionally averaged temperature biases are generally smaller than 1.5 °C. Building on these findings, Pieri et al. (2015) moved one step further, in the framework of the EXtreme PREcipitation and Hydrological climate Scenario Simulations (EXPRESS-Hydro) project, by dynamically downscaling at a finer space-time resolution (4 km, 3-hourly) the ERA-Interim dataset using the state-of-the-art non-hydrostatic Weather Research and Forecasting (WRF) regional climate model.

In this work the high-resolution ($\Delta t=3$ h, $\Delta x=4$ km) EXPRESS-HYDRO regional dynamical downscaling of historical climate scenarios is used as input to a hydro-meteorological chain

1   including a rainfall downscaling algorithm (RainFARM, Rebora et al. 2006a, 2006b) and a

2   continuous distributed hydrological model (Continuum, Silvestro et al. 2013). As a result, a

3   30-year long high resolution ($\Delta t=1$ h, $\Delta x=< 500$ m) hydrological dataset (e.g. Streamflow and

4   Evapotranspiration) was generated for a reference Mediterranean region. It is noteworthy to

5   highlight that both Continuum model and RainFARM downscaling algorithm have been

6   already widely employed and tested in the very same study area (Gabellani et al., 2008;

7   Silvestro et al., 2014; Laiolo et al., 2015; Davolio et al., 2017).

8   The distributed nature of the variables allowed to investigate the possibility of using the

9   hydrological modelling chain for extreme streamflow statistical analysis (e.g. distribution of

10   annual discharge maxima) and long-term water balance (e.g. long-term runoff ratio) with a

11   fully distributed approach. Furthermore, the fine space-time resolution of the forcings,

12   together with the use of a rainfall downscaling model, allowed to evaluate such a high

13   resolution reanalysis in regions featured with small hydrological watersheds (Silvestro et al.,

14   2011), complex topography and frequently flash-flooded (Altinbilek et al., 1997; Cassola et

15   al., 2016). The aforementioned elements, together with the analysis of the distribution of

16   flood extremes, are the main novel contributions of the presented analysis in respect to other

17   works that employ a similar modelling cascade: it is in fact mandatory to use high resolution

18   reanalysis since coarser ones cannot reproduce the small-scale rainfall structures that usually

19   trigger such local hydro-meteorological processes.(Buzzi et al., 2013; Marta-Almeida, 2016;

20   Pontoppidan et al. 2017; Schwitalla et al. 2017).

21   The study shows the capabilities and the limits of the considered modelling chain to

22   reproduce low-frequency streamflow and long-term water balance as an alternative to

23   observations in a scarce data environment or whenever a finer spatial distribution of hydro-

24   meteorological processes is essential.

The manuscript is organized as follows: section 2 describes the study area, hydro-meteorological data set and models, section 3 shows the results, and in section 4 the discussion and conclusions are reported.

2 Materials and Methods

2.1 Study Area and Case study

Liguria Region is located in northern Italy (Figure 1) and it is characterized by small (drainage are in the range 10-1000 km^2) and steep slope (10 - 20 %) basins (Table 1). The response time to precipitation is short, ranging between 0.5 and 10 hours (Maidment, 1992; Giannoni et al., 2005). The maximum elevation of mountains is around 2500 m, and most of the region is covered with forest or other types of vegetation like meadows and shrubs; usually the catchments mouths are densely urbanized. The hydrological regime is prevalently torrential and the entire study area is frequently hit by flash floods (Rebora et al., 2013): as a consequence, the variability of annual discharge maxima is high. Winter seasons are generally not rigid but, as the elevation varies from sea level to more than 2000 m, below-zero temperatures are rare (a few days ayear) along the coast and at low altitude but they can easily drops even below -10 °C inland. Snow occurs only few days a year and normally does not reach the coastal areas.

During warm season peak temperature hardly rises over 31-32 °C. The local raingauge network (OMIRL – "Osservatorio Meteo-Idrologico della Regione Liguria") is managed by the Environmental Agency of Liguria Region (ARPAL) and is quite dense (more than 150 gauges; 1 raingauge/40 km^2 on the average) ,with a 5-10 minute resolution and an homogeneous distribution with respect to the elevation. Temperature, radiation, wind, air humidity gauges are also part of the observational network, even though their density is lower, about 1/50, 1/200, 1/200, 1/60 km^2 respectively. The data seamlessly collected from 2011 to 2014 for calibrating/validating the hydrological model.

1   Besides, for a subset of 95 raingauge stations (see Figure 1), ARPAL hosts a web-based free-

2   access validated database of historical (1978 - 2010) daily precipitation measurements

3   (ARPAL, 2010) that were used in the present study for the bias correction of the EXPRESS-

4   Hydro reanalysis rainfall estimation.

5   For 11 level gauge stations seamless hourly data are available from 2011 to 2014 together

6   with rating curves, while annual discharge maxima (hereafter ADM) time series longer than

7   30 years are available for 15 level gauges (Figure 1); the latter ones cover sub-periods which

8   are not continuous from 1950 to recent years. Moreover, in the Hydrologic Annual Survey

9   (http://www.arpal.gov.it/homepage/meteo/pubblicazioni/annali-idrologici.html),   an   official

10   document published by ARPAL, annual basin-scale runoff ratio (defined as runoff

11   volume/precipitation) are available for 6 stations.

12   In Table 1 the availability of the discharge and discharge-related data is summarized together

13   with hydro-geomorphic characteristics of the basins upstream each station.

14   All the data are checked by ARPAL in compliance with WMO recommendations so as to flag

15   errors and unphysical values.

16

17   **2.2   Bias correction of rainfall fields (B.C.)**

18   Before being used as input for the hydrological simulations, the EXPRESS-Hydro reanalysis

19   rainfall dataset was compared with the climatological precipitation data of the Liguria

20   raingauge dataset (ARPAL, 2010). The observational dataset is constituted by validated time

21   series of about 95 raingauges homogeneously distributed on the Liguria Region territory,

22   covering the whole EXPRESS-Hydro dataset (not for all gauges, though) with a daily

23   timestep.

24   In order to provide Continuum the most reliable input data, the EXPRESS-Hydro reanalysis

25   precipitation data were bias-corrected with the actual raingauges so as to assure an accurate

1   reproduction of the local climatology in terms of monthly accumulation. As rainfall was the

2   only available data in the Liguria climatological atlas, the bias correction was not applied to

3   the other variables of the EXPRESS-Hydro dataset.

4   Nevertheless, several methods are available in literature to perform a bias correction

5   (hereafter B.C.) on different variables (e.g., rainfall, temperature, et c.; Fang et al. 2015):

6   amongst many, in this study a CDF-matching approach was selected (Fang et al. 2015).

7   In order to preserve the seasonality and the inter-annual variability which can be found in the

8   observational data as well as in the EXPRESS-Hydro ones, the correction was based on the

9   monthly accumulations. computed for both datasets. This led to generate 12 x N (where N is

10 the number of years of the dataset) maps of monthly-cumulated rainfall for Express-Hydro

11 and 12 x N_{obs} (being N_{obs} the number of years of the observed dataset) timeseries representing

12 the actual accumulated rainfall for each month and for each of the available raingauges.

13 To allow a direct comparison between the observed data and the modeled dataset, the monthly

14 cumulated data from the raingauges were previously interpolated on the Express-Hydro

15 spatial grid by using a kriging technique with a Spherical variogram. No regression with other

16 spatialized variables (e.g., elevation) was performed because previous tests showed no

17 significant correlation. Due to the high density of the raingauge network and since the

18 interpolation was applied only to the monthly accumulation, possible errors introduced by the

19 interpolation are assumed to be negligible as short-lived and small-scaled rainfall events ,

20 were addressed (see Boni et al., 2007 and Rebora et al. 2013).

21 For each cell i, the empirical CDF (Cumulative Distribution Function) of both observed and

22 modeled values were computed: with the purpose of minimizing the distortions, these CDFs

23 were calculated separately for each month of the year

1 In the CDF-matching process the observations CDF was applied to the Express-Hydro time

2 series of a given cell i in order to obtain the corrected time series of the monthly

3 accumulation:

4 $$PM'_{i,m} = F_{OSS,i}^{-1}\left(F_{MOD,i}\left(PM_{i,m}\right)\right) \qquad (1)$$

5 where PM is the Express-Hydro monthly accumulated rainfall, PM' is the bias-corrected

6 monthly accumulated rainfall, m is the index of the month of the native series, $F_{MOD,i}$ and

7 $F_{OSS,i}$ are respectively the CDF of the modeled and observed monthly rainfall in the cell i.

8 Given these corrected monthly time series, the single instantaneous value of rainfall p

9 (3-hours cumulate) was corrected as follows:

10 $$p'_{i,t} = p_{i,t}\frac{PM'_{i,m}}{PM_{i,m}} \qquad (2)$$

11 where:

12 - $p_{i,t}$ is the 3-hourly accumulated rainfall modeled in the cell i at time t

13 - $p'_{i,t}$ is the bias-corrected 3-hourly accumulated rainfall modeled in the cell i at time t

14 - $PM_{i,m}$ is the monthly accumulated rainfall modeled in the cell i for the month m (in

15 which the instant t falls)

16 - $PM'_{i,m}$ is the monthly accumulated rainfall modeled in the cell i for the month m (in

17 which the time t is) corrected with the CDF-matching

18 The described procedure allowed to obtain a 3-hourly maps dataset in which the model bias

19 was eliminated by keeping the characteristics of the modelled output in terms of seasonality

20 and inter-annual variability. Furthermore, the procedure allows to avoid alterations of possible

21 temporal trends, at both full-domain and single-cell spatial scale.

22 **2.3   Downscaling the rainfall with RainFARM Model**

23 RainFARM (Rebora et al. 2006a, 2006b) is a stochastic mathematical model that can be

24 exploited for generating downscaled rainfall fields consistent with the large-scale forecasts

25 provided by either Numerical Weather Prediction Systems (NWPs) as in Laiolo et al. (2013)

1   and by expert forecasters (Silvestro and Rebora, 2014). The model takes into account the

2   variability of precipitation at small spatial and time scales (e.g. L ≤ 1 km, t ≤ 1 hour),

3   preserving the precipitation volume at the scales considered reliable (L_r, and t_r) for

4   quantitative precipitation forecasts. In other words L_r, and t_r are those scales where we expect,

5   on average, a reliable forecast of precipitation volume. RainFARM is able on one side to

6   preserve spatial and time patterns at L_r, t_r, on the other side to produce small-scale structures

7   of rainfall which are consistent with detailed remote sensor observations as meteorological-

8   radar estimation (Rebora et al., 2006a).

9   In the model, the spatial-temporal Fourier spectrum of the precipitation is estimated using the

10   rainfall patterns predicted by a meteorological model and it is mathematically described as

11   follows:

12   $$\left| \hat{g}(k_x, k_y, \omega) \right|^2 \propto (k_x^2 + k_y^2)^{-\alpha/2} \omega^{-\beta} \qquad (3)$$

13   k_x and k_y are the x and y spatial wavenumbers, ω the temporal wavenumber (frequency),

14   while α and β are two parameters that are calibrated fitting the power spectrum of rainfall

15   derived by a NWPS on the frequencies corresponding to the spatial-time scales L_r, and t_r. By

16   extending the spectrum defined by equation (3) to the larger wave numbers/frequencies it is

17   possible to generate a spatial-time rainfall pattern at high resolution (Rebora et al. 2006b).

18   Since the Fourier phases related with the power spectrum (3) are randomly generated before

19   the backwards transformation in real space, RainFARM provides an ensemble of

20   equiprobable high-resolution fields that are consistent with the large-scale precipitation

21   forecastedby a NWPS. RainFARM was designed to feed flood forecasting systems in small

22   and medium sized basins (drainage area < 10^3-10^4 km^2) and it was widely tested on the study

23   area (Rebora et al., 2006a; Silvestro et al. 2012; Silvestro and Rebora, 2014).

1   In this study the algorithm is used to downscale the bias-corrected EXPRESS-Hydro

2   reanalysis; the nominal grid spacing and temporal resolution of EXPRESS-Hydro

3   precipitation (4 km and 3 hours, Hardenberg et al. 2015 and Pieri et al. 2015) are assumed as

4   reliable spatial and time scales. The downscaling algorithm is not used in probabilistic

5   configuration, but to build a possible rainfall time-spatial pattern at 1 km and 1 hour

6   resolution that is compatible with the runoff at small scales, since most of the catchments in

7   the study area are small-sized (often <100-200 km^2) with a response time ranging from 1 to 6

8   hours.

9   **2.4   The hydrological model and its calibration-validation**

10   2.4.1   The model: Continuum

11   The hydrological model used in this study is *Continuum* (Silvestro et al. 2013), a distributed

12   and continuous model that relies on a space-filling approach and uses a robust way for the

13   identification of the drainage network components (Giannoni et al., 2005). Though all the

14   main hydrological processes are mathematically described in a distributed way, Continuum

15   was designed to be a trade-off between complex physically-based models (which describe the

16   physical phenomena with a high detail, often introducing complex parameterization) and

17   models with a empirical approach (easy to implement but not accurate enough, Silvestro et

18   al., 2015). The basin or domain of interest is represented through a regular grid, derived by a

19   Digital Elevation Model (DEM) while the flow directions are defined with an algorithm that

20   calculates the maximum slope using the DEM. An algorithm classifies each cell of the

21   drainage network as hillslope or channel flow depending on the main flow regime; a

22   morphologic filter is defined by the expression $AS^k = C$ where A is the drainage area

23   upstream of each cell [L^2], S is the local slope [-], k and C are constants related to the

24   geomorphology of the catchment (Giannoni et al., 2000) and it is used to determine whether a

25   cell is a hillslope or a channel. The surface flow scheme treats differently channel and

1 hillslope flows: the overland flow (hillslopes) is described by a linear reservoir

2 schematization, while an approach derived by kinematic wave (Wooding, 1965; Todini and

3 Ciarapica, 2001) models the channel flow.

4 Subsurface flows and infiltration are modeled through an adaptation of the Horton equations

5 (Bauer, 1974; Disikin and Nazimov, 1997) that accounts for soil moisture evolution even in

6 conditions of intermittent and low-intensity rainfall as in Gabellani et al. (2008).

7 Interception of vegetation is schematized with a reservoir that has a retention capacity S_v

8 estimated by static informative layers of vegetation type or Leaf Area Index data; the flow in

9 deep soil and the water table evolution are modeled with a distributed linear reservoir

10 schematization and a simplified version of Darcy equation.

11 The energy balance uses the "force restore equation" (Dickinson, 1988) that allows to

12 explicitly model the soil surface temperature and to estimate the evapotranspiration from the

13 latent heat flux (Silvestro et. al 2013).

14 Snow melting and accumulation is simulated with simple equations forced with air

15 temperature and solar radiation (Maidment, 1992) as in Silvestro et al. (2015).

16 Continuum needs the following input variables: rainfall, air temperature, short-wave solar

17 radiation, wind velocity, and relative humidity. When the ExpressHYDRO reanalysis are used

18 to feed the model the input variables are: 2m temperature, 10 m wind, rain depth, downward

19 short wave flux at ground surface, and 2 m relative humidity

20 The parameters that require calibration in Continuum model are six, they are often estimated

21 at basin or sub-basin scale: two for the surface flow (u_h [$m^{0.5}s^{-1}$] and u_c [s^{-1}]), two for the sub-

22 surface flow (c_t [-] and c_f [-]) and two for deep flow and watertable (V_{Wmax} [mm] and R_f [-])

23 processes.

24 The parameter u_h affects those hydrograph components which are related to fast surface flow

25 as well as u_c but the impact of the latter depends on the length of the channeled paths; c_f is

1 related to saturated hydraulic conductivity and controls the rate of subsurface flow rate (i.e.,

2 it); c_t identifies the part of water volume in the soil that can be extracted through

3 evapotranspiration only and is thus related to the soil field capacity, while both c_t and c_f

4 regulate the dynamics of saturation of the root-zone. The two parameters V_{Wmax} and R_f

5 control the flow in the deep soil and the dynamic of watertable, yet they impact on recession

6 curves and influence flood hydrographs only when large-sized catchments are taken into

7 account (Silvestro et al., 2013).

8 ### 2.4.2 Implementation on the study area

9 In the present work, Continuum was implemented with a time resolution of 60 minutes and a

10 spatial resolution of 0.005 deg (about 480 m). The Shuttle Radar Topographic Mission

11 (SRTM) DEM was employed as a terrain model.

12 The model was calibrated on 11 basins where streamflow observations were available at

13 hourly time resolution (see Table 1); the hourly measurements of rainfall, air temperature,

14 solar radiation, air relative humidity provided by the regional weather stations network were

15 interpolated on a 1-km regular grid through a Kriging method to feed the model. The two

16 parameters V_{Wmax} and R_f were estimated at regional scale based also on Davolio et al. (2017),

17 since they are less sensitive than the other four parameters (Silvestro et al., 2013). The

18 observed streamflow data at 60-minute time resolution were compared with the model output

19 in order to evaluate its performance. The validation period spanned from 01/01/2013 to

20 31/12/2014, the model performance was evaluated through the skill scores, also used in the

21 calibration process (Davolio et al., 2017), as reported in the following .

22 The Nash Sutcliffe (NS) coefficient (Nash and Sutcliffe, 1970):

23 $$NS = 1 - \sum_{t=1}^{t\,max} \frac{\left(Q_m(t) - Q_o(t)\right)^2}{\left(Q_m(t) - \overline{Q_o}\right)^2}$$ (4)

1   where $Q_m(t)$ and $Q_o(t)$ are the modelled and observed streamflows at time t. $\overline{Q_o}$ is the mean

2   observed streamflow.

3   Relative Error of High Flows (REHF)

4    $$REHF = \frac{1}{t\max}\left[\sum_{t=1}^{t\max}\frac{|Q_m(t)-Q_o(t)|}{Q_o(t)}\right]_{Q>Qth}$$ (5)

5   where Q_{th} is chosen as the 99 percentile of the observed hydrograph along the calibration

6   period.

7   While NS has the purpose of evaluating the general reproduction of streamflow, REHF score

8   aims to give more weight to the highest flows thus leading the calibration to better reproduce

9   the flood events.

10   As in Madsen (2000) the calibration was carried out by combining NS and REHF into a

11   multi-objective function: the space parameter was analyzed using a brute force approach on

12   the time span 2011-2013 in order to optimize the aforementioned multi-objective function.

13   The time resolution of the streamflow data was hourly, while the Curve Number map was

14   derived by the CORINE Land Cover (http://www.sinanet.isprambiente.it/it/progetti/corine-

15   land-cover-1). The parameters range values considered during the calibration process were

16   defined considering their physical meaning, the mathematical constraints and the experience,

17   they are reported in Table 2 (Silvestro et al., 2015; Cenci et al., 2016), the final parameter

18   configuration is similar to the one used in Davolio et al. (2017).

19   The values of the skill scores were calculated for the validation period and turned out to be

20   satisfactory, as reported in Table 3.

21   For those basins where the calibration was not possible, the parameters are assumed to be

22   equal to the average values obtained by the calibration. This assumption was then verified by

23   carrying out a run of the model using the average parameters even for calibrated basins; the

1 statistics maintain good values supporting the significant assumption done. Table 3 reports the

2 skill scores.

3 Even if the calibration of the model did not encompass all the study region due to the lack of

4 data, the hydrological model (as well) was proven to be as performing as similar models

5 specifically developed for the same study area (Giannoni et al., 2000, 2005; Gabellani et al.,

6 2008; Silvestro et al. 2013, 2015; Cenci et al 2016), even for flood forecasting in not

7 calibrated sections (Regione Marche, 2016). In fact, when the basins have similar

8 characteristics especially regarding the surface response to intense rainfall and the main

9 genesis of rainfall-runoff process, the parameters have often similar values (Boni et al., 2007).

10 In order to reduce the warm up impacts on the 1979 (first year of EXPRESS-Hydro)

11 simulation, a first run was started with a predefined initial condition setup and the state

12 variables simulated on the 31 of December of every year (from 1979 to 2008) were averaged

13 to estimate a reasonable initial condition for 1th January 1979 to be used in the final

14 simulation.

15 The hydrological model run for the period 1979-2008 provided, a streamflow time series for

16 each pixel of the calculation domain which was, ideally, equivalent to having a gauge every

17 Δx along the hydrological network. Since the spatial resolution of the hydrological model is

18 480 m basins smaller than A_{th}=15 km^2 were not taken into account , because the surface water

19 motion processes cannot be modeled with a sufficient detail (Giannoni et al., 2005).

20 **2.5   Distribution of the annual discharge maxima**

21 The results of the modeling chain were firstly compared with observations using a typical

22 station-wise comparison approach: 15 gauge stations with at least 30 years of annual

23 discharge maxima (ADM) were identified along the Ligurian territory from east to west.

24 It was not possible to ensure a perfect overlapping between the simulated and the

25 observational timeseries, often observed data are not seamless and they may cover longer

1   periods (in some case 50-60 years) with large timespans of missing data. However, on the

2   basis of the conclusions drawn in the Liguria climatological atlas, major climate change-

3   related trends for the meteorological variables are not evident, thus allowing for the use of the

4   database despite the data gaps.

5   The comparison between observed and reanalysis-driven ADM is firstly based on the analysis

6   of the respective cumulative density function distributions.

7   The reanalysis-driven ADM were fitted with a Generalized Extreme Value (GEV) distribution

8   (see e.g., Hoskin and Wallis, 1993; Piras et al., 2015) that represents a good compromise

9   between flexibility and robustness. Other works based extreme statistical analysis on the Two

10   Components Extreme Value (TCEV) model (Rossi et al., 1984), nevertheless we decided to

11   use GEV since it has a smaller number of parameters and it was widely applied (CIMA

12   Research Foundation, 2015; Piras et al., 2015). Moreover the comparison between observed

13   and modeled ADM was also done using the Kolmogorov-Smirnov test with a 5% significance

14   level, in order to verify if they belonged to the same distribution.

15   **2.6   Regional analysis of the annual discharge maxima**

16   In order to carry out a comparison following a distributed approach we referred to Boni et al.

17   (2007) which is one of the operational reference methods in Liguria Region (used by both

18   public authorities and private engineers) to estimate the ADM quantiles (Provincial Authority

19   of Genoa, 2001; Silvestro et al., 2012). The method was conceived and tested especially for

20   the Tyrrhenian catchments of Liguria Region, so the present analysis was carried out only for

21   this area; the 45-50% of which is located upstream the calibrated basins. The method defines

22   a hierarchical approach based on the analysis of the non-dimensional random variable $X_0 =$

23   X/μ_x, obtained by grouping together all the available data, and making them non-dimensional

24   with respect to each local (gauging station) sample mean, μ_x, taken as the index flood for

25   gauged sites. Index flood is estimated even where observations were not available by taking

15

advantage of the rainfall regional frequency analysis and rainfall-runoff modelling to allow

quantile estimation in each point of the region.

The final result is a methodology to estimate the index flood that can be formalized as it

follows:

$$Q_{index} = f(Area, longitude) \qquad (6)$$

While the quantile is:

$$Q(T) = K(T) \cdot Q_{index} \qquad (7)$$

where T is the return period and K(T) is defined by the non-dimensional regional growth

curve, uniquely defined for all the studied region (Boni et al. 2007).

In the case of the modelling chain analyzed in this work a large number of reanalysis-driven

time series is available because 30 year long ADM series for each pixel of the model grid can

be accessed for basins bigger than A_{th}. In practice, using a distributed hydrological model, on

one side allows the index flood estimation to be a simple mean of a time series in each point

of the domain, on the other side provides a large number of data to build the non-dimensional

regional curve.

3   Results

3.1   Precipitation analysis

The comparison between EXPRESS-Hydro reanalysis and precipitation climatology over

Liguria derived from observational data was undertaken at annual, seasonal, monthly and

daily scales.

Pieri et al. (2015), using EURO4M-APGD reference observational dataset (Isotta et al. 2013,

with about 50 daily raingauge stations in Liguria), already showed an overall underestimation

of the WRF rainfall depths on annual basis, more evident on the eastern side of the region

(Figure 3, panels e-f of Pieri et al. 2015), with differences in the range between -2 and -1

1 mm/day on the eastern coastal part and between -1 and 0 mm/day on the eastern Apennines

2 side.

3 The same analysis was repeated and extended in this study, using 95 raingauges in Liguria:

4 results on annual rainfall depth confirm the findings of Peri et al. (2015) both on eastern and

5 western Liguria sides (Figure 2).

6 Concerning the seasonal results, EXPRESS-Hydro tends to underestimate average observed

7 rainfall depths during DJF (Figure 3) on eastern Liguria (between 0-100 mm) while generally

8 overestimates them on centre-west (0-100 mm); the same holds also for MAM (Figure 3).

9 During JJA, instead, EXPRESS-Hydro underestimation ranges between 0 and 100 mm over

10 both the western and eastern sides, while ramps up to 100 - 200 mm over the centre. The

11 underestimation deepens over eastern Liguria during SON (Figure 3), with values between -

12 100 and 200 mm inland and up to 200 - 300 mm over the coast. Conversely, on the rest of the

13 region the underestimation drops between 0 -100 mm. In Figure 4 the seasonal comparison

14 between observations and EXPRESS-Hydro is also shown in terms of scatter plots, with a

15 good correlation between reanalysis and observations, while in Table 4 we reported the values

16 of bias and Root Mean Square Error (RMSE).

17 Figure 5 shows the box plot of monthly precipitation averaged at regional scale for both

18 EXPRESS-Hydro and observations, obtained by the averaging the maps of accumulated

19 rainfall. The comparison highlights that EXPRESS-Hydro satisfyingly reproduces the

20 variability along the 30 years, but often underestimates the rainfall amount; particularly in

21 January, September and October.

22 Figure 6 shows the same analysis of Figure 5 but at catchment scale on 4 basins whose

23 characteristics are reported in Table 1; the basins locations was spread from east to west side

24 of the region to investigate if different behaviours arise along the study area. It is interesting

1   to evidence that while a general underestimation of rainfall during fall period is found for the

2   rivers located in central-east Liguria (Entella closed at Panesi and Vara closed at Nasceto),

3   the other 2 test basins behave rather differently as the box plots of Argentina closed at Merelli

4   and Arroscia closed at Pogli show an overestimation during spring, especially in April and

5   May.

6   A further analysis was carried out in order to understand how EXPRESS-Hydro reanalysis

7   reproduces the rainfall annual maxima, especially after the application of bias correction;

8   ADM of the region are in fact generally driven by very intense rainfall events that have

9   duration lower or equal to 24 hours. We thus compared the annual maxima of 24 hours

10   accumulated rainfall (ARM) derived by observations with those derived by the reanalysis

11   (with B.C.) again following the approach described in Boni et al. (2007): each series of ARM,

12   observed and modeled, was normalized with its average and a regional non-dimensional

13   distribution function was built. The result is reported in Figure 7 which shows a very good fit

14   between observations and reanalysis, this confirms a general good reproduction of the

15   climatology even in terms of ARM.

16   **3.2   Distribution of the annual discharge maxima**

17   In Figures 8 to 10 a selection of observed and reanalysis-driven ADM CDF distributions, the

18   GEV and the corresponding 95% confidence intervals are shown. Six basins were chosen in

19   order to evidence the variability of results, showing either good and poor performances,

20   moreover the comparisons are referred to hydrological gauging stations where reliable and

21   long-time series of observed ADM are available. For each station the results obtained with

22   and without rainfall B.C. are both reported.

23   The cases in Figure 8 show a shift of the observed distribution with respect to the modeled

24   one especially without B.C. Low ADM observed values lay out of the confidence intervals of

the reanalysis-driven ADM GEV distribution, while the most extreme values fall inside the confidence intervals. The distributions without bias correction show an underestimation of ADM; B.C. led to very good results for Entella closed at Panesi and to an overestimation on Bisagno closed at La Presa case.

Magra closed at Piccatello (Figure 9) shows an overestimation in both cases, even higher after the B.C; Argentina closed at Merelli benefits of B.C. especially regarding the extreme ADM values.

Arroscia closed at Pogli shows an improvement of reanalysis-driven ADM, once B.C. is performed, while Nervia ADM without B.C. well fits the observations and B.C. leads to an overestimation (Figure 10).

The Kolmogorov-Smirnov test with a 5% significance level on ADM was applied to all the selected stations and the corresponding results are summarized in Table 5. It is interesting that bias correction does not allow to increase the number of null-hypothesis (data belong to the same distribution) yet: 9 stations out of 15 pass the test either B.C. is applied or not. Changing the significance level does not affect the final findings in a significant way: with a 1% 12 stations pass the test with B.C. and 11 without B.C., with 10% 7 stations pass the test with B.C. and 7 without B.C.. This fact could derive on how the B.C. -acting on the monthly volume- affects the short-lived and severe rainfall events that usually are responsible for the ADM in many parts of the study area.

The poor reproduction of ADM in some sections may be due to various causes; on one side it was not possible to calibrate the model over the whole study region, on the other side in some periods and in some sub-regions the rainfall reanalysis is probably poorly representative of actual rainfall and B.C. does not correct it enough. Moreover observed peaks and simulated peaks are often referred to different time periods: this, together with the typical hydro-climatic

19

1   regime of the study region (flash floods with high variability of ADM) could have a

2   significant impact on final results.

3   We would like also to highlight the fact that simulated ADM distributions have often similar

4   shapes to the observed ones and suffer of a sort of bias (for example Bisagno closed at La

5   Presa, Figure 8), while in other cases the simulated ADM distribution is only partially out of

6   the confidence intervals (example Argentina closed at Merelli, Figure 9). The average

7   hydrologic regime on the study region could be only partially affected by the local bad fittings

8   of ADM.

9   **3.3   Regional analysis of the annual discharge maxima**

10   Figure 11 shows the comparison between the non dimensional regional growth curve obtained

11   fitting a GEV on simulated ADM computed with and without B.C., the observations

12   (available ADM on Liguria Region) and the simulated ADM. The results are quite good even

13   if it seems that the modeling chain without B.C. leads to a small underestimation of high

14   frequency events (low T) and a small overestimation of low frequency events (high T) with

15   respect to the observations. Anyway both observed and modeled ADM lay inside the

16   confidence intervals (95 %) for a large part of the curve.

17   In the Figure we reported the curves built using simulations of all the sections with a drainage

18   area larger than A_{th} together with those obtained using only the sections where the

19   hydrological model was calibrated. The curves that used only calibrated sections are really

20   similar to the others, proving that the latter configuration enhances the robustness of the

21   regional curve estimation without introducing evident errors.

22   The main differences in the case of B.C. configuration are that observations lay always inside

23   the confidence intervals and there is a better matching between simulated and observed

24   sample curves. This is a significant finding in fact the regional curve is an important

25   ingredient to deal with quantile estimation in ungauged sections. It is important to highlight

1   that regional approach allows to reduce the errors that can be found for single basins (Boni et

2   al., 2007) and which are shown in section 3.2; on one side the normalization of each ADM

3   series with its average reduces the effects of bias (due for example to a bad hydrological

4   model calibration), on the other side the ADM time series of each outlet section (or grid

5   point) is only a small sub-sample of the entire sample used to build the regional curve.

6   To compare the quantiles estimated using the modelling chain with those in Boni et al. (2007)

7   the following ratio was considered:

8   $$Ratio(T) = \frac{Q(T)_{Model}}{Q(T)_{Reg}} \qquad\qquad (8)$$

9   where Model and Reg respectively stand for modelling chain and regional analysis, T is the

10 return period, Q is the ADM. Ideally, if the modelling chain provided exactly the same results

11 of the benchmark regional analysis, the Ratio(T) value should be around 1, Ratio(T) > 1 (<1)

12 means overestimation (underestimation).

13 Figure 12 shows Ratio(T) for T=2.9 years (Index Flow) as a function of the drainage area (A

14 in km^2), while Figure 13 shows the maps of Ratio(T) for T=2.9 years and T=50 years.

15 The first consideration is that a relation between Ratio(T) and A appears to exist, probably

16 because the chain is not able to reproduce in detail the meteorological and hydrologic

17 processes at very fine time and spatial scales (Siccardi et al., 2005), in fact for A < 30-50 km^2

18 the underestimation seems quite systematic even if B.C. improves results. Ratio(T) is

19 generally underestimated also for A>30-50 km^2 but B.C. generally leads to a better balance

20 between over- and underestimation, despite introducing the overestimation grows on larger

21 basins (A > 200-300 km^2). From Figure 13 a general improvement driven by B.C. stands out

22 especially in those areas where the model chain without B.C. underestimates Q(T). Areas

23 where modelling chain is really close to the benchmark are in green/light blue, whereas dark

24 blue and purple point out where under or overestimation is high (absolute difference larger

1   than 70-100%); noticeably, Ratio(T) for T= 50 years and T=2.9 years (Figure 13) have a

2   similar pattern.

3   In central Liguria the Ratio(T) obtained with EXPRESS-Hydro leads to results comparable

4   with Boni et al. (2007) regardless the use of B.C., while simulations with B.C. are affected by

5   overestimation. This could be due to different causes: i) EXPRESS-Hydro is likely to well-

6   reproduce the events at small time and spatial scales (3-6 hours, 10-100 km^2) in that part of

7   the region as well as generally underestimates monthly asccumulation, in this case B.C. could

8   lead to streamflow overestimation; ii) the hydrological model may need a better calibration,

9   but it does not seem the most probable option; in fact B.C leads to the overestimation of ADM

10   even in calibrated basins, this occurrence arose even in the site comparison (Bisagno creek,

11   see section 3.2) iii) the quantiles in this area may have been underestimated by Boni et al.

12   (2007). It has to be noticed that overestimation is larger for T=2.9 years than for T=50 years

13   (see Figure 13, some basins are in purple for T=2.9 years and in yellow-orange for T=50

14   years), this is probably due to the fact that the shape of the growing curve in the B.C. case

15   leads to a reduction of the overestimation as T increases; the behaviour on western Liguria is

16   similar to the centre even if less stressed and evident for larger basins only.

17   The underestimation on smaller catchments (A < 30-50 km^2) could be partially due to a not

18   optimal parameterization of the hydrological model (especially where calibration was not

19   possible), but it appears more reasonable that the errors related to parameterization would lead

20   to a uniform-like distribution between over and underestimation. However, the model spatial

21   resolution could play a role since the representativeness of the catchment morphology

22   decreases for small drainage areas with a general smoothing effect that affects the results: this

23   degradation effect is clearly continuous from large to small drainage areas, though a threshold

24   for the analysis (i.e., basins with Area<16 km^2 are neglected) was set.

A further cause is presumably that EXPRESS-Hydro cannot always adequately reproduce the rainfall structures at fine spatial and temporal scale, and the downscaling procedure can only partially correct this drawback. Moreover the time resolution (1 hour after downscaling) could be not sufficient when drainage area is small (Silvestro et al., 2016; Rebora et al., 2013): as a consequence, the runoff processes needed to trigger such very small catchments are not properly modelled (Siccardi et al., 2005).

The combination of the aforementioned factors leads us to conclude that the underestimation of quantiles for very small catchments (i.e. A < 30-50 km^2) is a structural problem of the modelling chain.

This fact is supported by the analysis shown in Figure 14, left panel. The Ratio(T) averaged on the target area is plotted as a function of T for all the sections with drainage Area ≥ 16 km^2. Ratio increases with T especially for the B.C. case, meaning that the growth curve values K(T) obtained by EXPRESS-Hydro partially balance the underestimation of average ADM (used as Index Flow) in the estimation of higher quantiles; Ratio(T=2.9 years) changes from 0.47 to 0.71, Ratio(T=50 years) from 0.45 to 0.66. If the threshold area is increased from 16 to 50 km^2 (Figure 14, right panel) the underestimation drops for both cases, with and without B.C..

As already shown, the general underestimation of Ratio(T) for small catchments is not completely confirmed for all the region, for instance, in part of central Liguria results are quite good even for basins with Area < 50 km^2 and bias correction leads to an overestimation of Ratio(T). Apparently, in this area EXPRESS-Hydro can produce rainfall with a spatial-temporal structure able to trigger floods compatible with the hydro-climatology of local small basins. This is also the part of the study region that previous studies demonstrated to be characterized by the highest values of rainfall maxima for 1, 3, 6, 12 and 24 hours (Boni et al., 2008).

1 **3.4 Effects of the rainfall downscaling on simulated ADM**

2 In order to assess the influence of the rainfall downscaling, the modelling chain was applied

3 without it. In this way for each pixel of the domain a 30year long time series of ADM was

4 computed by the hydrological model driven with the bias-corrected rainfall reanalysis at

5 EXPRESS-Hydro native resolution. The rainfall field was assumed to have a constant

6 intensity over 3-hourly timestep and resampled from 4 km to 1 km.

7 The 30-year average ADM was computed and compared to the ones obtained by the complete

8 chain by estimating the following ratio for each grid cell:

9 $$RatioDS = \frac{Q_{MeanNoDS}}{Q_{MeanDS}} \qquad\qquad (9)$$

10 where $Q_{MeanNoDS}$ (Q_{MeanDS}) is the average ADM obtained without (with) downscaling. The

11 RatioDS was then plot versus the drainage area as in Figure 15:the downscaling impact

12 generally increases as the drainage area decreases, and it is crucial to simulate the ADM on

13 small catchment when drainage area is lower than 100-150 km^2. Moreover RatioDS is always

14 lower than 1, thus confirming that rainfall downscaling enhances the runoff formation as in

15 Siccardi et al. (2005), likewise the analysis evidences how the underestimation of quantiles

16 shown in section 3.3 would worsen without it.

17 **3.5 Water balance and runoff ratio**

18 In this section some considerations about the long-term water balance are shown in order to

19 evaluate how the applied system can reproduce the hydrological cycle and the variables

20 related to water balance and water resources management.

21 Taking advantage of the modelled evapotranspiation maps, the distributed runoff ratio (RR) at

22 cell scale is estimated as:

23 $$RR(x,y) = \frac{Rain(x,y) - Evt(x,y)}{Rain(x,y)} \qquad\qquad (10)$$

1   where Rain(x,y) and Evt(x,y) are the modeled total rainfall and evapotranspiration in the cell

2   with coordinates (x,y) over the 30 years of simulation. The maps of RR are shown in Figure

3   16, together with the maps of mean annual rainfall for both cases with and without B.C..

4   The spatial pattern of RR is strongly correlated to the precipitation one, and the latter is in

5   turn evidently related with orography, especially for the case without B.C..

6   When a single cell has a large number of upstream cells, it tends to be frequently saturated

7   because of the contributions of subsurface flow of the upstream cells: the values in the cells

8   that belong to channel network as simulated by the hydrological model (Giannoni et al., 2005)

9   are not shown because they are hardly representative (generally, the values are very low or

10   even negative).

11   B.C. produces an increasing of both precipitation and runoff ratio on the entire region and a

12   reduction of the differences between coastal and inland areas. In order to estimate how the

13   modeling chain reproduces the available observations the runoff ratio at basin scale on a

14   target section S is computed by:

15   $$Rs(s) = \frac{VQ(s)}{Rain(s)} \qquad\qquad (11)$$

16   where Rain(s) is the accumulated rainfall over the basin laying upstream the section S and

17   VQ(s) is the integral on time of the streamflow volume passed through the section S. We

18   considered some closure sections where the runoff ratio estimated by observations (rainfall

19   and streamflow) is available (see Table 1) from the Hydrologic Annual Survey

20   (http://www.arpal.gov.it/homepage/meteo/pubblicazioni/annali-idrologici.html), an official

21   document published by the Regional Agency for Environment Protection. The observed

22   runoff ratios are not available for the simulation period (1979-2008) but they are estimated as

23   an average of the values measured in non-continuous periods since 1940s to present, thus

24   providing a possible benchmark to assess the performance of the modeling chain.

1 Modeled RRs are compatible with the hydro-climatology of the target area (Barazzuoli and

2 Rigati, 2004; Provincia di Imperia, 2017) but at the same time it is evident a general

3 underestimation in the western part of the region (basins 4,5,6); B.C. improves results and

4 RRs are more similar to the benchmark (Table 6.).

5 The rainfall B.C. introduces only small variations in terms of runoff ratio, thus meaning that

6 when the long term water balance is addressed, the increasing or decreasing of rainfall lead on

7 similar percent variation on both runoff and evapotranspiration.

8 For example, in the central and eastern parts of Liguria, B.C. generally increases the

9 precipitation and reduces the orographic features of the spatial pattern, but at the same time

10 the evapotranspiration increases too, consequently RRs rise is small. As shown in sections 3.2

11 and 3.3 the increasing of rainfall leads to larger values of ADM, but the RRs do not change

12 significantly: this could be due to the fact that other EXPRESS-Hydro variables that influence

13 the energy balance (and the long term water balance) like solar radiation or wind speed may

14 benefit a correction, nevertheless no reliable and dense data are available for the entire

15 simulation period. Another approach could be to perform a calibration more focused to

16 preserve long term runoff. In any case we could say that generally the results are good and

17 they highlight the potentialities of using such modeling chain even for water balance

18 purposes.

19 **4   Discussion and conclusions**

20 This work explores the possibility of using EXPRESS-Hydro, a high-resolution regional

21 dynamical downscaling of ERA-Interim dataset by means of the state-of-the-art non-

22 hydrostatic Weather Research and Forecasting (WRF) regional climate model for

23 hydrological purposes on small catchments. This was done by feeding a distributed

24 continuous hydrological model with a subset of the EXPRESS-Hydro meteorological

25 variables to produce streamflow simulations; the rainfall fields were downscaled from the

native space-time resolution (4km, 3 hours) to a finer one (1km, 1 hour) before they were used to feed an hydrological model. All the analyses were conducted either applying and not applying a bias correction to rainfall fields. The study area is Liguria, a Region in the north-western Italy, with a particular focus on its Tyrrhenian coast.

Firstly we evaluated the performance of the modelling chain in reproducing extreme streamflow statistics by following two methods: i) by comparing statistical distribution of ADM with observations in some gauging points ii) by using as a benchmark the regional analysis presented in Boni et al. (2007) that allows a comparison with a distributed approach. We then evaluated how the modeling chain reproduces the long term water balance by analyzing the modeled runoff ratios and using as a benchmark the estimations based on observations.

The results are encouraging even if the modelling chain cannot always meet the considered benchmarks with high accuracy. The ADM statistic is quite good in most of the target region but in some sub-regions the quantiles are sometimes under- or over-estimated. Rainfall B.C. generally improves the underestimation, yet introducing an overestimation in some basins especially in the central part of the region and in the largest basins.

A single-site comparison of modelled and observed ADM shows that, for a large number of the gauging sites the time series belong to the same distribution with a 5% significance, the fitting of modelled ADM with GEV distributions is generally good and often the observations lay inside the 95% confidence interval, especially for low-frequency quantiles. It must be noted that anyway in some sites the GEV fitting without B.C. is better than that with B.C.

A comparison with the regional analysis shows interesting results as the behaviour remarkably drifts in some parts of the region, depending on how EXPRESS-Hydro generates the spatial-temporal patterns of precipitation and how much rainfall bias correction is effective.

1   Both point and distributed analysis show that there is a general underestimation for basins

2   with drainage area smaller than 30-50 km^2 but B.C. is able to tackling it largely. This is

3   probably due to structural problems of the modelling chain under the aforementioned size:

4   for those basins it is necessary to further refine the time and spatial scales of the

5   meteorological input (precipitation chiefly, Siccardi at al., 2006; Silvestro et al., 2016), and

6   likely of hydrological model too (Yang et al., 2001). A possible way to deal with very small

7   basins is to better exploit the potentialities of the downscaling algorithm (RainFARM) that is

8   here used in a deterministic way to generate a possible time (1-hour)- and space (1km) pattern

9   with the constraint of maintaining the precipitation volumes and structures generated by

10   EXPRESS-Hydro at its native resolution (3 hours, 4 km).

11   Runoff ratio RR was used to evaluate long term water balance. The RR coefficient evaluated

12   on a 30-year long simulation period at cell scale reasonably meets the climatology of the

13   region (Barazzuoli and Rigati, 2004; Provincia di Imperia 2017) and its pattern is highly

14   correlated with annual mean rainfall distribution. RR at basin scale was compared with

15   observations-based estimates for some gauging points and the values are of the same order of

16   magnitude, however the modelling chain generally underestimates in both configurations

17   even if B.C. results are slightly better. This could be due to the fact that also the variables

18   related to energy balance (for example the solar radiation and wind) modelled by EXPRESS-

19   Hydro probably need a correction, but this analysis was not carried out, mainly for the lack of

20   reliable and sufficiently dense data.

21   To summarize this work, the present modelling chain was proven to reliably simulate the

22   hydro-meteorological statistics in the study area, even if some difficulties and gaps were

23   emphasized by the study. The fully distributed approach allows to reproduce the hydro-

24   climatic characteristics and features in a seamless way over the whole territory. Rainfall B.C.,

25   by helping the system to better model some characteristics not completely captured even by a

high-resolution meteorological reanalysis, contributes in a relevant way to improve the results even in very small basins (Area < 30-50 km^2) generally affected by structural underestimation.

References

Altinbilek, D., Barret, E. C., Oweis, T., Salameh, E., Siccardi, F.: Rainfall Climatology on the Mediterranean, EU-AVI 080 Project ACROSS—Analyzed climatology rainfall obtained from satellite and surface data in the Mediterranean basin. EC Rep. A VI2-CT93-080, 32pp, 1997.

ARPAL. http://www.arpal.gov.it/homepage/meteo/analisi-climatologiche/atlante-climatico-della-liguria.html. (last access: 12 October 2017), 2010.

Asadieh, B., Krakauer N. Y.: Global change in streamflow extremes under climate change over the 21st century Hydrol. Earth Syst. Sci., 21, 5863–5874, 2017. https://doi.org/10.5194/hess-21-5863-2017

Barazzuoli P., Rigati R.: studio per la definizione del bilancio idrogeologico del bacino del fiume Magra. http://www.adbmagra.it/Pdf/UNISI_Bil_Idr_Magra_Rel_Fin.pdf Università degli studi di Siena. 2004. Last access date: 2017/03/02

1   Bastola S., Misra V.: Evaluation of dynamically downscaled reanalysis precipitation data for

2   hydrological application. Hydrol. Process., Published online in Wiley Online Library

3   (wileyonlinelibrary.com) DOI: 10.1002/hyp.9734, 2013.

4   Bauer, S.: A modified Horton equation during intermittent rainfall. Hydrol. Sci. Bull., 19,

5   219–229, 1974.

6   Berenguer, M., Corral, C., Sanchez-Diesma, R., and Sempere-Torres, D.: Hydrological

7   validation of a radar-based nowcasting technique. Journal of Hydro-Meteorology, 6, 532-549,

8   2005.

9   Boni, G., Ferraris, L., Giannoni, F., Roth, G., Rudari, R.: Flood probability analysis for un-

10   gauged watersheds by means of a simple distributed hydrologic model. Advances in Water

11   Resources, 30(10), 2135-2144, 2007, doi:10.1016/j.advwatres.2006.08.009.

12   Boni, G., Parodi, A., Siccardi, F.: A new parsimonious methodology of mapping the spatial

13   variability of annual maximum rainfall in mountainous environments. Journal of

14   Hydrometeorology, 9(3), 492-506, 2008.

15   Buzzi, A., Davoilio, S., Malguzzi, P. Drofa, O., Mastrangelo, D.: Heavy rainfall episodes over

16   Liguria of autumn 2011: numerical forecasting experiments. Nat. Hazards Earth Syst. Sci.

17   Discuss., 1, 7093–7135, 2013.

18   Borga, M.: Accuracy of radar rainfall estimates for streamflow simulation. J. Hydrol., 267,

19   26–39, 2002.

20   Calanca, P., Roesch, A., Jasper, K., Wild, M.: Global warming and the summertime

21   evapotranspiration regime of the Alpine region, *Clim. Change*, 79(1–2), 65–78. 2006.

22   Cassola, F., Ferrari, F. Mazzino A., Miglietta, M.M.: The role of the sea on the flash floods

23   events over Liguria (northwestern Italy). Geophys. Res. Lett. 43, 3534–3542,2016.

1   Cenci L., Laiolo P., Gabellani S., Campo L., Silvestro F., Delogu F., Boni G., and Rudari R.,

2   Assimilation of H-SAF Soil Moisture Products for Flash Flood Early Warning Systems. Case

3   Study: Mediterranean Catchments. IEEE Journal of Selected Topics in Applied Earth

4   Observations and Remote Sensing, vol. 9, no. 12, pp. 5634-5646, Dec. 2016. DOI:

5   10.1109/JSTARS.2016.2598475

6   Choi, W., Kim, S. J., Rasmussen, P.F., Moore, A. R., Canadian Water Resources Journal.

7   Vol. 34(1): 17–36, 2009.

8   CIMA Foundation (2015), GAR (2015), Improvement of the Global Flood model for the

9   GAR 2015, Input Paper prepared for the Global Assessment Report on Disaster Risk

10 Reduction 2015.

11 Davolio, S., Silvestro., F., Malguzzi, P. : Effects of Increasing Horizontal Resolution in a

12 Convection Permitting Model on Flood Forecasting: The 2011 Dramatic Events in Liguria

13 (Italy). J. Hydrometeor. , 16, 1843-1856, 2015. doi:10.1175/JHM-D-14-0094.1.

14 Davolio, S., Silvestro, F., Gastaldo, T.: Impact of rainfall assimilation on high-resolution

15 hydro-meteorological forecasts over Liguria (Italy). J. Hydrometeor., 18, 2659-2680, 2017.

16 https://doi.org/10.1175/JHM-D-17-0073.1

17 De Michele, C., Rosso, R., A multi-level approach to flood frequency regionalisation.

18 Hydrology and Earth System Sciences, 6(2), 185–194, 2002.

19 Dickinson, R.: The force-restore method for surface temperature and its generalization,

20 Journal of Climate, 1:1086-1097, 1988.

21 Diskin, M. H., Nazimov, N.: Linear reservoir with feedback regulated inlet as a model for the

22 infiltration process, J. Hydrol., 172, 313–330, 1994.

23 Döll, P., Müller S: How is the impact of climate change on river flow regimes related to the

24 impact on mean annual runoff? A global-scale analysis. Environ. Res. Lett. 7 (11pp). 2012

1   Fang, G. H., Yang, J., Chen, Y. N., Zammit, C.: Comparing bias correction methods in

2   downscaling meteorological variables for a hydrologic impact study in an arid area in China.

3   Hydrology and earth System Sciences, 19, 2547-2559, 2015.

4   Fu, G., Charles, S. P., Viney, N. R. Chen, S. L., Wu J. Q.: Impacts of climate variability on

5   stream-flow in Yellow River. Hydrol. Processes, 21(25), 3431–3439, 2007.

6   Gabellani, S., Silvestro, F., Rudari, R. and Boni, G.: General calibration methodology for a

7   combined Horton-SCS infiltration scheme in flash flood modelling. Nat. Hazards Earth

8   Science, 8, 1317 - 1327, 2008.

9   Kottegoda, N.T., Rosso R.: Statistics, Probability, and Reliability for Civil and Environmental

10 Engineers. McGraw-Hill Companies, New York, 1997.

11 Krogh, S.; Pomeroy, J.W.; Mcphee, J.P. Physically based mountain hydrological modeling

12 using reanalysis data in patagonia. J. Hydrometeorol. 16, 172–193, 2015.

13 Giannoni, F., Roth., G., and Rudari, R.: A Semi – Distributed Rainfall – Runoff Model Based

14 on a Geomorphologic Approach. Physics and Chemistry of the Earth, 25/7-8, 665-671, 2000.

15 Giannoni, F., Roth, G. Rudari, R.: A procedure for drainage network identification from

16 geomorphology and its application to the prediction of the hydrologic response. Advances in

17 Water Resources, 28(6), 567-581, 2005, doi:10.1016/j.advwatres.2004.11.013.

18 von Hardenberg, J., Parodi, A., Pieri, A. B., & Provenzale, A.: Impact of Microphysics and

19 Convective Parameterizations on Dynamical Downscaling for the European Domain. In

20 Engineering Geology for Society and Territory-Volume 1 (pp. 209-213), 2015. Springer

21 International Publishing.

22 Hersbach, H.: Decomposition of the continuous ranked probability score for ensemble

23 prediction systems. Weather and Forecasting 15: 559–570, 2000.

24 Hosking, J.R.M., Wallis, J.R.: Some statistics useful in regional frequency analysis. Water

25 Resourc. Res., 29, 271-281, 1993

Isotta, F. A., and Coauthors: The climate of daily precipitation in the Alps: Development and analysis of a highresolution grid dataset from pan-Alpine rain-gauge data. Int. J. Climatol., 34, 1657–1675, doi:10.1002/joc.3794, 2013.

Kotlarski, S., Keuler, K., Christensen, O. B., Colette, A., Déqué, M., Gobiet, A., Nikulin, G.: Regional climate modeling on European scales: a joint standard evaluation of the EURO-CORDEX RCM ensemble. Geoscientific Model Development, 7(4), 1297-1333, 2014

Laiolo, P., Gabellani, S., Rebora, N., Rudari, R., Ferraris, L., Ratto, S., Stevenin, H. Cauduro, M.: Validation of the Flood-PROOFS probabilistic forecasting system. Hydrol. Process., 28: 3466–3481, 2014. doi: 10.1002/hyp.9888

Laiolo P., Gabellani S., Campo L., Silvestro F., Delogu F., Rudari R., Pulvirenti L., Boni G., Fascetti F., Pierdicca N., Crapolicchio R., Hasenauer S., Puca S.: Impact of different satellite soil moisture products on the predictions of a continuous distributed hydrological model. International Journal of Applied Earth Observation and Geoinformation. doi:10.1016/j.jag.2015.06.002.Madsen, H.: Automatic calibration of a conceptual rainfall–runoff model using multiple objectives, Journal of Hydrology, 235, 276–288, 2000.

Maidment, D., (1992), Handbook of Hydrology. McGraw-Hill, Inc.

Marta-Almeida, M., Teixeira, J. C., Carvalho, M. J., Melo-Gonçalves, P., & Rocha, A. M. (2016). High resolution WRF climatic simulations for the Iberian Peninsula: model validation. Physics and Chemistry of the Earth, Parts A/B/C, 94, 94-105.

Molini, L., Parodi, A., Siccardi F.: Dealing with uncertainty: an analysis of the severe weather events over Italy in 2006, Nat. Hazards Earth Syst. Sci., 9, 1-13. 2009.

Nkiaka, E.; Nawaz, N.R.; Lovett, J.C. Evaluating Global Reanalysis Datasets as Input for Hydrological Modelling in the Sudano-Sahel Region. *Hydrology. 4*, 13, 2017.

Pieri, A. B., von Hardenberg, J., Parodi, A., Provenzale, A.: Sensitivity of Precipitation Statistics to Resolution, Microphysics, and Convective Parameterization: A Case Study with

the High-Resolution WRF Climate Model over Europe. Journal of Hydrometeorology, 16(4), 1857-1872, 2015.

Piras, M., Mascar, G., Deidda, R., Vivoni, E. R.: Impacts of climate change on precipitation and discharge extremes through the use of statistical downscaling approaches in a Mediterranean basin. *Sci. Total Environ.*, http://dx.doi.org/10.1016/j.scitotenv.2015.06.088., 2015

Pontoppidan, M., Reuder, J., Mayer, S., & Kolstad, E. W.: Downscaling an intense precipitation event in complex terrain: the importance of high grid resolution. Tellus A: Dynamic Meteorology and Oceanography, 1271561, 2017.

Provincia di Imperia: Piano di bacino stralcio sul bacino idrico del torrente Arroscia. http://pianidibacino.provincia.imperia.it/Portals/_pianidibacino/Documents/Cap%20_4.pdf Last access date: 2017/03/02.

Provincial Authority of Genoa: River basin planning of the Bisagno creek. http://cartogis.provincia.genova.it/cartogis/pdb/bisagno, 2001.

Rebora, N., L., Ferraris, J. H., Hardenberg and Provenzale, A.: Rainfall downscaling and flood forecasting: a case study in the Mediterranean area. Nat. Hazards and Earth Syst. Sci., **6**, 611-619, 2006a.

Rebora, N., Ferraris, L., Hardenberg, J. H. and Provenzale, A.: The RainFARM: Rainfall Downscaling by a Filtered Auto Regressive Model. Journal of Hydrometeorology, 7(4), 724-738, 2006b.

Rebora, N., Molini, L., Casella, E., Comellas, A., Fiori, E., Pignone, F., Siccardi, F., Silvestro, F., Tanelli, S., Parodi, A.: Extreme Rainfall in the Mediterranean: What Can We Learn from Observations? J. Hydrometeorol., 14, 906-922, 2013.

1 Regione Marche. -Regionalizzazione delle portate massime annuali al colmo di piena per la

2 stima dei tempi di ritorno delle grandezze idrologiche. http://www.regione.marche.it/Regione-

3 Utile/Protezione-Civile/Progetti-e-Pubblicazioni/Studi-Meteo-Idro#Studi-Idrologici-e-

4 Idraulici. 2016. Last access date: 19/10/2017Rossi F, Fiorentino M, Versace P.: Two

5 component extreme value distribution for flood frequency analysis. Water Resour Res.

6 20(2):847–56, 1984.

7 Schwitalla, T., Bauer, H. S., Wulfmeyer, V., & Warrach-Sagi, K.: Continuous high-resolution

8 midlatitude-belt simulations for July–August 2013 with WRF. Geoscientific Model

9 Development, 10(5), 2031, 2017.

10 Siccardi, F., Boni, G., Ferraris, L. and Rudari, R.: A hydro-meteorological approach for

11 probabilistic flood forecast. J. Geophys. Res, 110, d05101, doi:10.1029/2004jd005314, 2005.

12 Silvestro, F., Gabellani, S., Giannoni, F., Parodi, A., Rebora, N., Rudari, R., Siccardi, F.: A

13 Hydrological Analysis of the 4th November 2011 event in Genoa. Nat. Hazards earth syst.

14 Sci., 12, 2743-2752, 2012, doi:10.5194/nhess-12-2743-2012.

15 Silvestro, F., Rebora, N. and Ferraris, L.: Quantitative flood forecasting on small and medium

16 size basins: a probabilistic approach for operational purposes. Journal of Hydrometeorology,

17 12(6), 1432-1446, 2011.

18 Silvestro, F., Gabellani, S., Delogu, F., Rudari, R., Boni, G.: Exploiting remote sensing land

19 surface temperature in distributed hydrological modelling: the example of the Continuum

20 model. Hydrol. Earth Syst. Sci., 17, 39-62, 2013. doi:10.5194/hess-17-39-2013.

21 Silvestro, F., Rebora, N.: Impact of precipitation forecast uncertainties and initial soil

22 moisture conditions on a probabilistic flood forecasting chain. Journal of Hydrology 519,

23 1052–1067, 2014.

24 Silvestro, F., Gabellani, S., Delogu, F., Rudari, R., Laiolo, P., Boni,, G.: Uncertainty

25 reduction and parameter estimation of a distributed hydrological model with ground and

remote-sensing data, Hydrol. Earth Syst. Sci., 19, 1727-1751, 2015, doi:10.5194/hess-19-1727-2015

Silvestro, F., Rebora, N., Giannoni, F., Cavallo, A., Ferraris, L.: The flash flood of the Bisagno Creek on 9th October 2014: an "unfortunate" combination of spatial and temporal scales. Journal of Hydrology, 541, Part A, Pages 50–62, 2016, doi:10.1016/j.jhydrol.2015.08.004

Stanki, H.R., Wilson, L.J., Burrows, W.R.: Survey of common verification methods in meteorology, Technical report No. 8 Geneva: WMO, 1989.

Todini, E., Ciarapica, L.: The TOPKAPI Model. Mathematical Models of Large Watershed Hydrology. In: Singh, V. P. et al. (eds) Water Resources Publications, Littleton, Colorado, Chapter 12, 2001.

Trinh, B. N., Thielen-del Pozo, J., Thirel, G.: The reduction continuous rank probability score for evaluating discharge forecasts from hydrological ensemble prediction systems. Atmospheric Science Letters, 14(2), 61-65, 2013.

Vieux, B. E., Bedient, P. B.: Assessing urban hydrologic prediction accuracy through event reconstruction. J. Hydrol., 299, 217–236, 2004.

Wooding, R. A.: A hydraulic modeling of the catchment-stream problem. 1. Kinematic wave theory, *Journal of Hydrology*, 3, 254–267, 1965.

Yang, D., Herath S., Musiake K.: Spatial resolution sensitivity of catchment geomorphologic properties and the effect on hydrological simulation. Hydrol. Process. 15, 2085–2099, 2001, DOI: 10.1002/hyp.280

5 Tables

Basin	Section	ADM 30 years time series	Hourly discharge data	Runoff ratio	Area [km^2]	Mean Slope [%]	Mean heght [m]
Magra	Calamazza	X	X		1650	18	503
Magra	Piccatello	X		X	78	21	590
Vara	Nasceto	X	X	X	202	23	651
Petronio	Riva Trigoso	X			55	19	401
Graveglia	Caminata	X			43	24	590
Entella	Panesi	X	X	X	364	21	535
Lavagna	San Martino	X			163	23	570
Bisagno	Passerella Firpo		X		92	20	398
Bisagno	La Presa	X			34	25	520
Sansobbia	Ponte Poggi	X			33	21	470
Neva	Cisano	X	X	X	123	25	670
Arroscia	Pogli	X	X	X	204	27	650
Impero	Rugge	X			73	19	480
Argentina	Merelli	X	X	X	188	26	883
Nervia	Isolabona	X			123	22	690
Tanaro	Ponte Nava	X			147	23	1350

Bormida	Murialdo		X		134	19	820
Bormida	Piana Crixia		X		273	15	550
Orba	Tiglieto		X		76	21	560
Aveto	Cabanne		X		33	23	1130

1 Table 1: availability of discharge data used for model validation, ADM analysis, long term

2 mass balance analysis. The characteristics of the basins upstream each measurement station

3 are reported.

4

Parameter	u_c [m$^{0.5}$s^{-1}]	u_h [s^{-1}]	c_t [-]	c_f [-]	V_{Wmax} [mm]	R_f [-]
Range	20-150	0.0001-0.001	0.1-0.7	0.005-0.1	200-1500	0.5 10

2   Table 2: ranges of parameter values considered for the calibration-validation process.

3

4

Basin	Section	u_c [m$^{0.5}$s^{-1}]	u_h [s^{-1}]	c_t [-]	c_f [-]	NS	REHF	NS (AP)	REHF (AP)
Magra	Calamazza	127	0.000194	0.3	0.05	0.81	0.14	0.75	0.34
Vara	Nasceto	125	0.000191	0.5	0.035	0.83	0.10	0.79	0.17
Entella	Panesi	64	0.000192	0.3	0.05	0.77	0.18	0.69	0.28
Bisagno	Passerella Firpo	110	0.000556	0.5	0.05	0.26	0.16	0.24	0.21
Neva	Cisano	63	0.000194	0.3	0.05	0.71	0.25	0.59	0.47
Arroscia	Pogli	65	0.000192	0.3	0.02	0.74	0.31	0.66	0.39
Argentina	Merelli	62	0.000185	0.3	0.035	0.84	0.21	0.78	0.3
Bormida	Murialdo	85	0.000174	0.3	0.05	0.35	0.51	0.21	0.87
Bormida	Piana Crixia	66	0.000200	0.5	0.02	0.76	0.41	0.57	0.35
Orba	Tiglieto	114	0.000278	0.5	0.02	0.88	0.21	0.84	0.29
Aveto	Cabanne	69	0.000520	0.5	0.02	0.73	0.41	0.77	0.45

Table 3: hydrological model validation; skill score values obtained for the calibrated. The calibrated parameters are also reported. V_{Wmax} [mm] and R_f [-] have values 500 mm and 1 for all the basins.

1

	BIAS [mm]	RMSE [mm]
DJF	-10.47	60.21
MAM	-0.71	56.13
JJA	-47.71	59.58
SON	-89.55	120.73

2 Table 4: Comparison between seasonal rainfall observations and EXPRESS-Hydro. Skill

3 scores estimated on seasonal time scale.

4
5
6

1
2
3
4

Basin	Section	P value	K-S test	P value (B.C.)	K-S test (B.C.)
Magra	Calamazza	0.008	NO	0.855	Yes
Magra	Piccatello	0.036	NO	0.021	NO
Vara	Nasceto	0.632	Yes	0.012	NO
Petronio	Riva Trigoso	0.780	Yes	0.023	NO
Graveglia	Caminata	0.030	NO	0.065	Yes
Entella	Panesi	0.002	NO	0.990	Yes
Lavagna	San Martino	0.062	Yes	0.701	Yes
Bisagno	La Presa	0.056	Yes	0.022	NO
Sansobbia	Ponte Poggi	0.350	Yes	0.005	NO
Neva	Cisano	0.420	Yes	0.110	Yes
Arroscia	Pogli	0.172	Yes	0.820	Yes
Impero	Rugge	0.003	NO	0.860	Yes
Argentina	Merelli	0.078	Yes	0.218	Yes
Nervia	Isolabona	0.206	Yes	0.449	Yes
Tanaro	Ponte Nava	0.001	NO	0.034	NO

5 Table 5: Kolmogorov-Smirnov test with 5% significance. P values are reported together with

6 verification of null-hypothesis (data belong or not to the same distribution).

7
8
9
10
11

1
2
3

Basin	Section	N. Progr	Area [km^2]	Obs. RR.	Model RR	Model RR (B.C.)
Magra	Piccatello	1	78	0.61	0.62	0.63
Vara	Nasceto	2	202	0.7	0.64	0.66
Entella	Panesi	3	364	0.73	0.64	0.67
Neva	Cisano	4	123	0.59	0.47	0.49
Arroscia	Pogli	5	204	0.55	0.48	0.51
Argentina	Merelli	6	188	0.65	0.51	0.53

4 Table 6. Runoff ratios (RR) obtained by the modeling chain (with and without the

5 rainfall bias correction) compared to those estimated by observations.

6
7
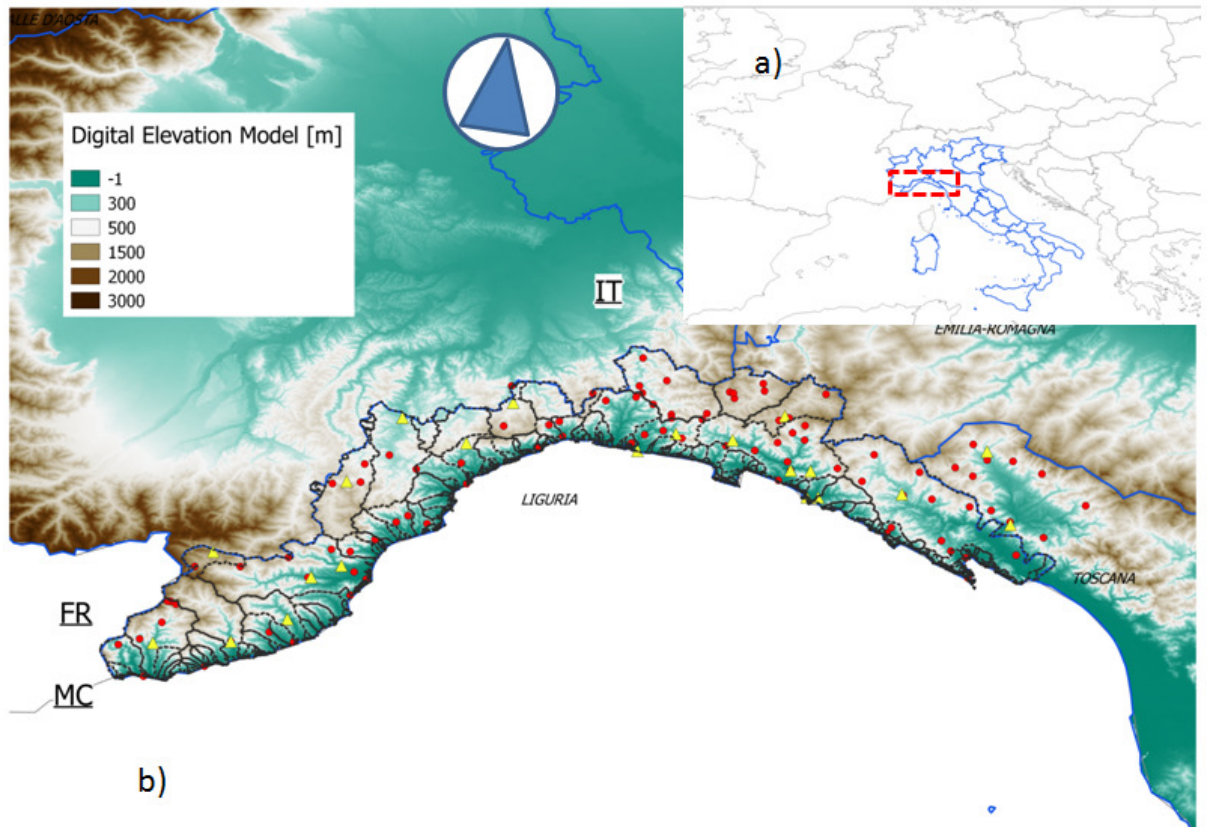
6 Figures

Figure 1. Study area geo-location at large scale (a) and zoom (b). Blue lines represent the regional boundaries of Italy, dashed line shows the main catchments of the study region, red dots represent the meteorological rain-gauge station of Liguria region of Italy where 32 years (1978-2010) of daily data are available, yellow triangles are the level gauge sections. Digital elevation model highlights the morphology of the region. In the bottom right corner the curve number map is reported to show synthetically the usage of soil.
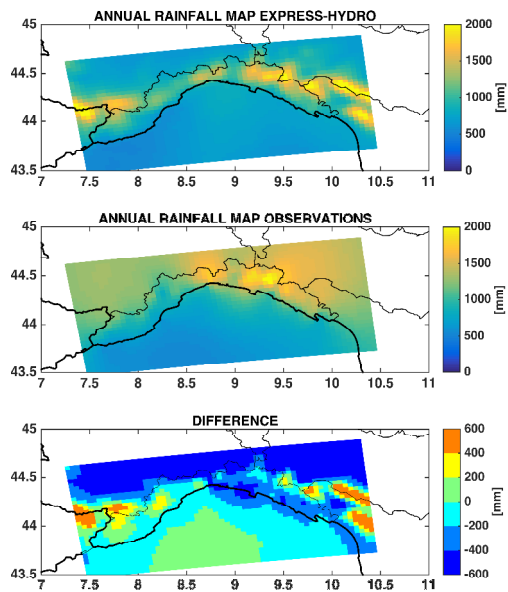
Figure 2. Upper panel shows the average annual rainfall map over Liguria area, the middle panel shows the average observed annual rainfall map, while the bottom one shows their difference in mm.

1
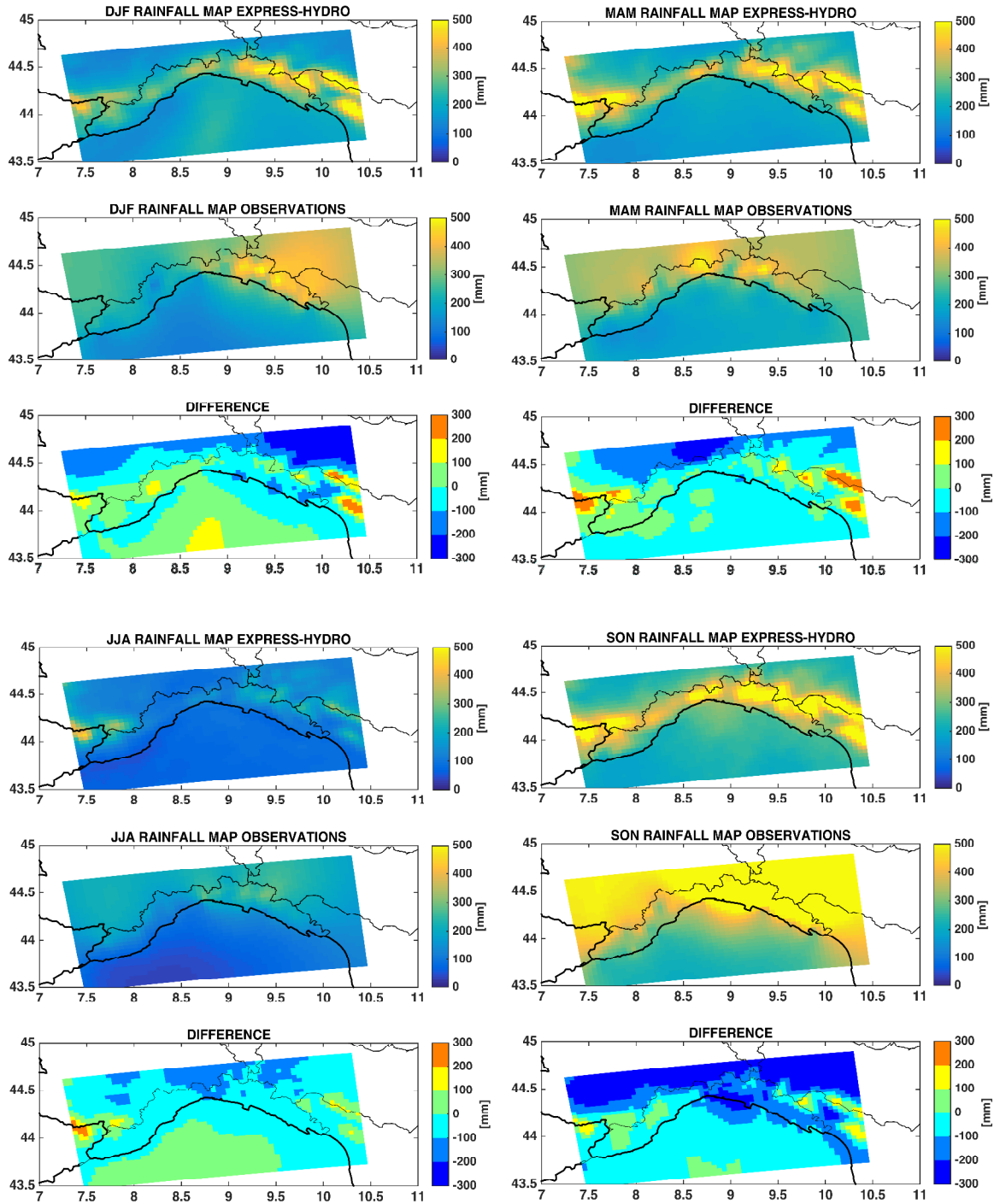
Figure 3. Upper panel shows the average DJF, MAM, JJA, SON rainfall maps over Liguria. For each season 3 maps are shown: EXPRESS-Hydro rainfall map, observed rainfall map, difference map in mm.

6

1
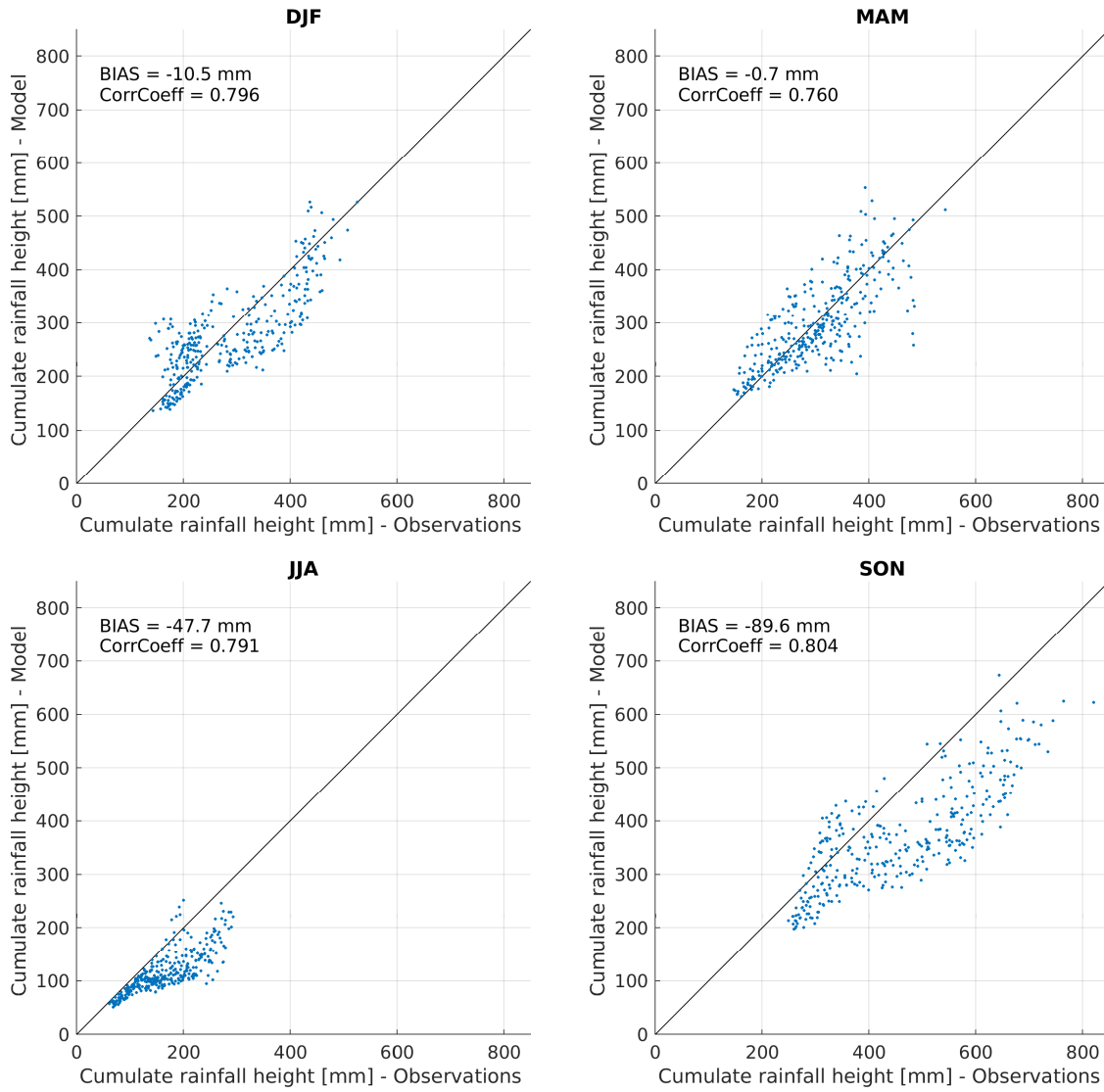
2

3 Figure 4: Scatter plots of seasonal precipitation built using data on EXPRESS-Hydro spatial

4 resolution (pixel to pixel comparison). X axis reports observed interpolated rainfall, Y axis

5 reports EXPRESS-Hydro estimation.

6

7

8

1

Monthly cumulate rainfall distribution - Observations (blue), Express-Hydro (red)
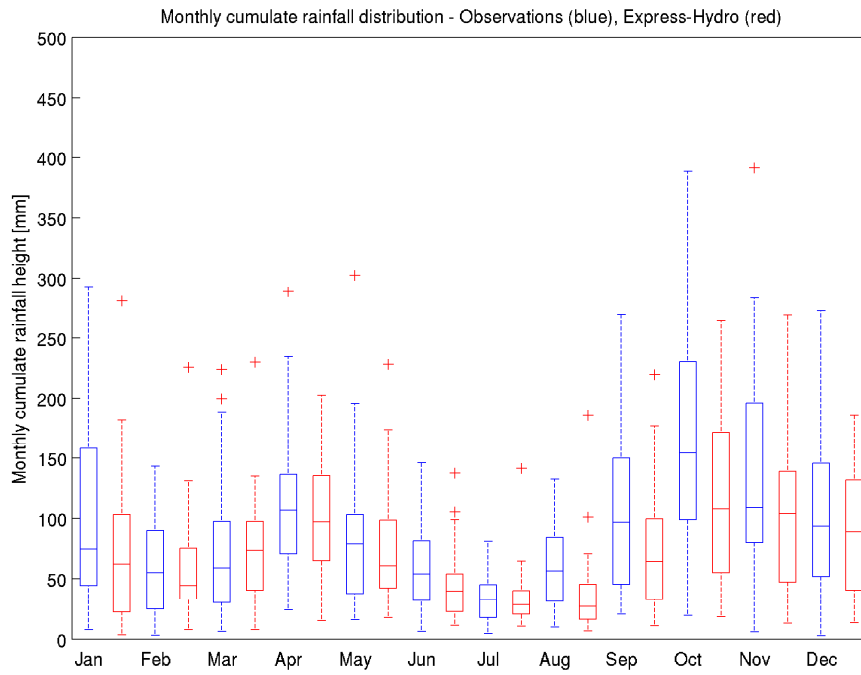
2

3   Figure 5: Box plot of monthly precipitation averaged at regional scale. Blue box plots are

4   built with observations while red ones with EXPRESS-Hydro reanalysis.

5

1

2
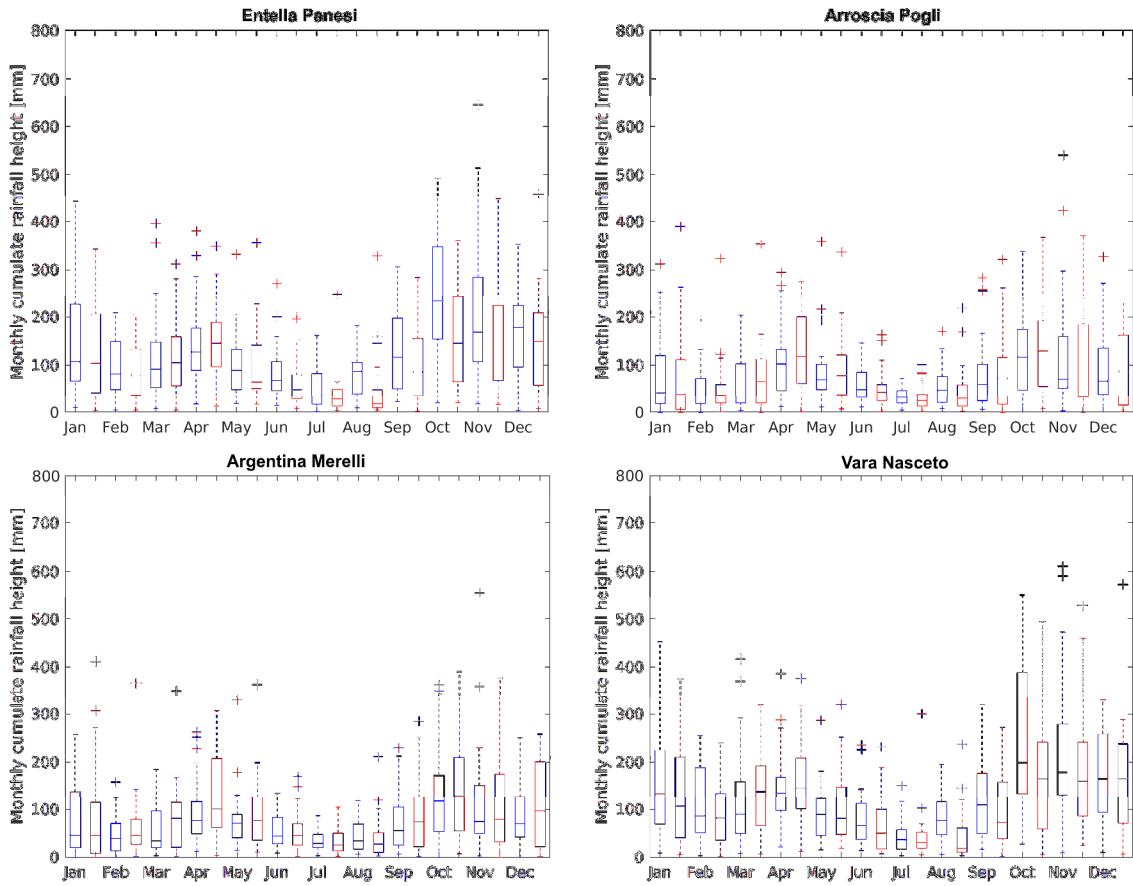
Figure 6: Box plot of monthly precipitation averaged at basin scale for 4 test catchments. Blue

box plots are built with observations while red ones with EXPRESS-Hydro reanalysis.

5

1
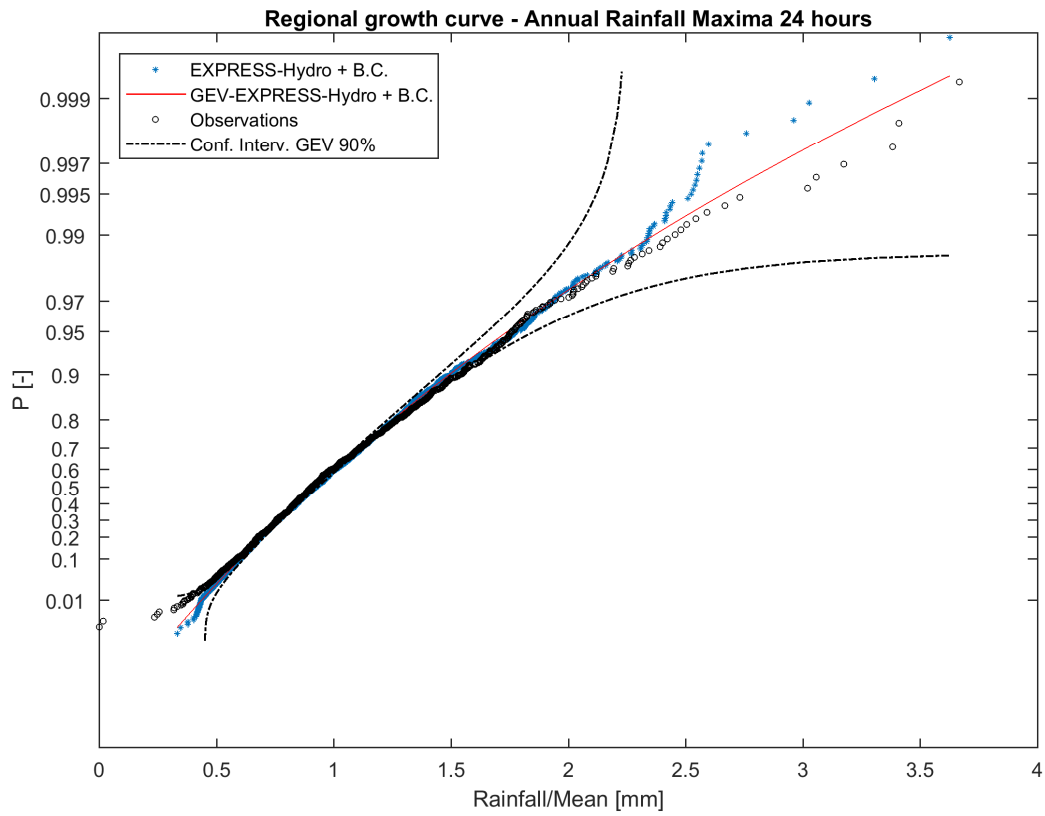
Figure 7. Growth curve obtained by annual maxima of 24 hours accumulated rainfall. Observations (blue dots) compared with EXPRESS-Hydro reanalysis (black dots). Red line is the GEV distribution fitted on EXPRESS-Hydro values while dotted lines are the confidence intervals with significance 95%

2

3

4

5

6

7

1

2

3
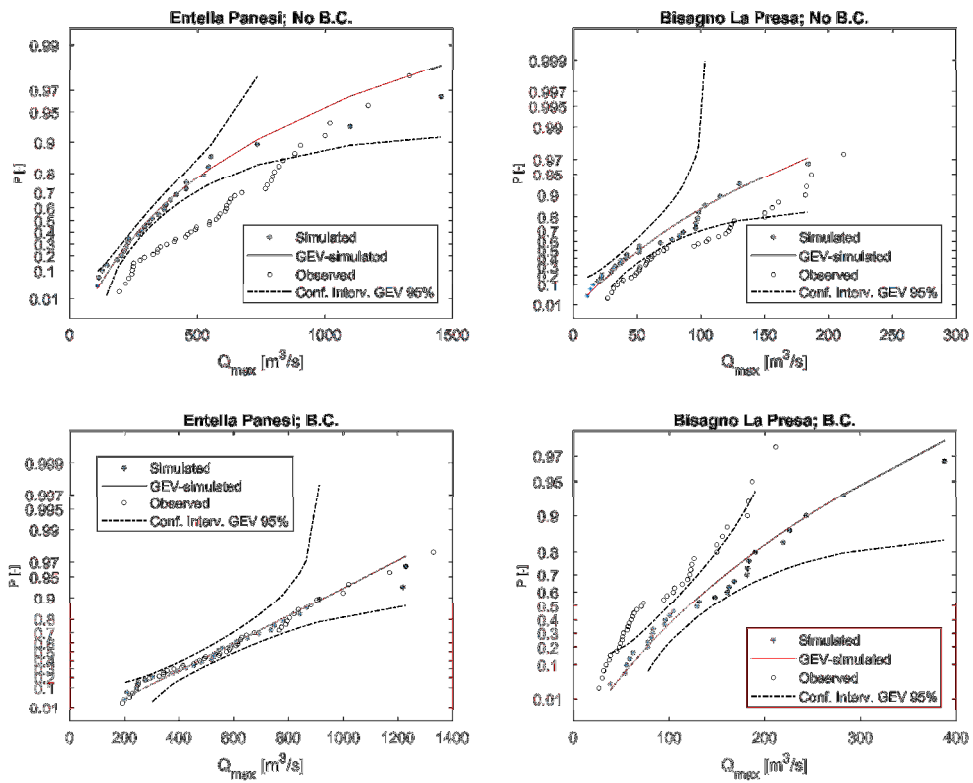
4 Figure 8. Distribution of ADM for Entella closed at Panesi (364 km^2) and Bisagno

5 closed at La Presa (34 km^2). Blue dots are the simulated ADM, black dots are observed

6 ADM, red line is the GEV fitted on simulated ADM while dotted lines are confidence

7 intervals with 95% significance. Upper panels show results without rainfall bias

8 correction, bottom panels show results with rainfall bias correction.

9

10
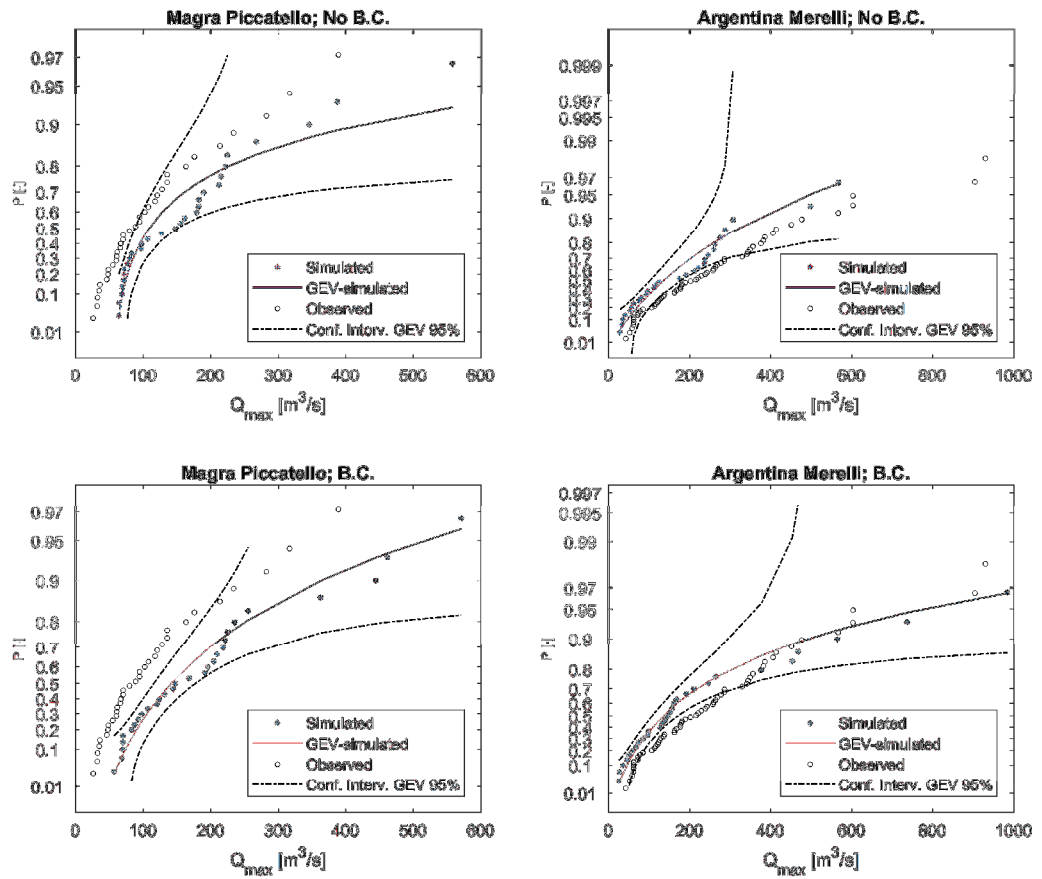
1

2   Figure 9. Same as figure 8 but for Magra closed at Piccatello (78 km^2) and Argentina

3   closed at Merelli (188 km^2).
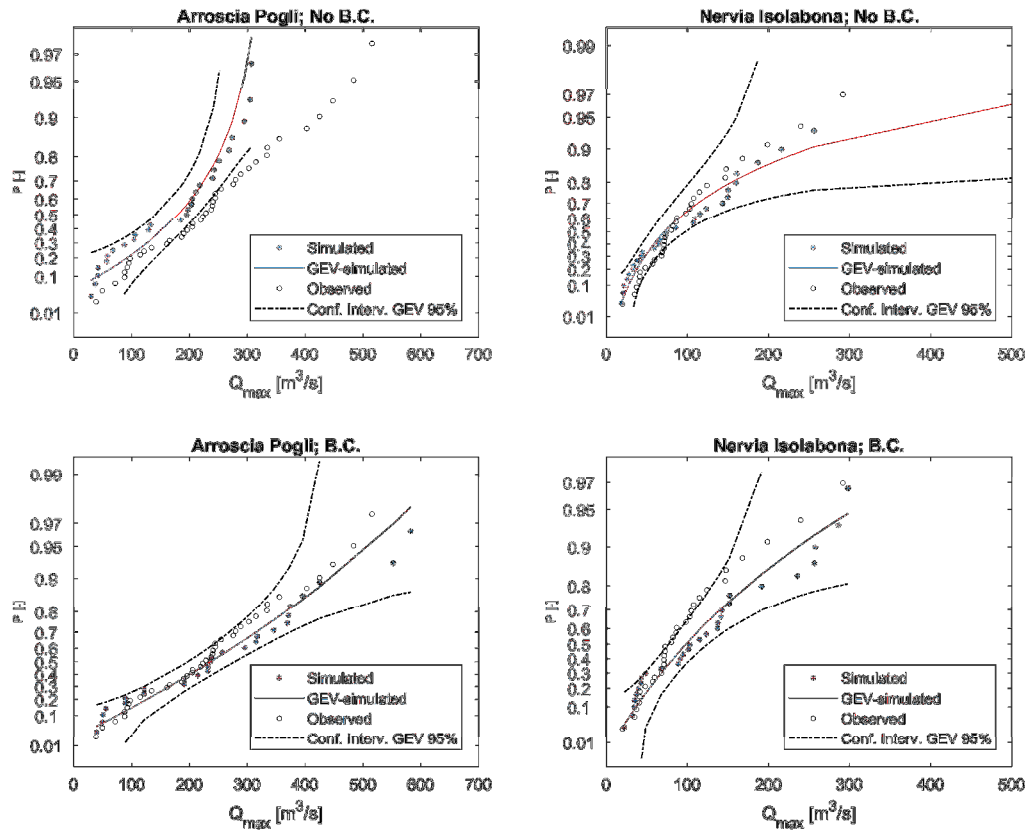
Figure 10: Same as figure 8 but for Neva closed at Cisano (123 km^2) and Nervia closed at Isolabona (122 km^2).
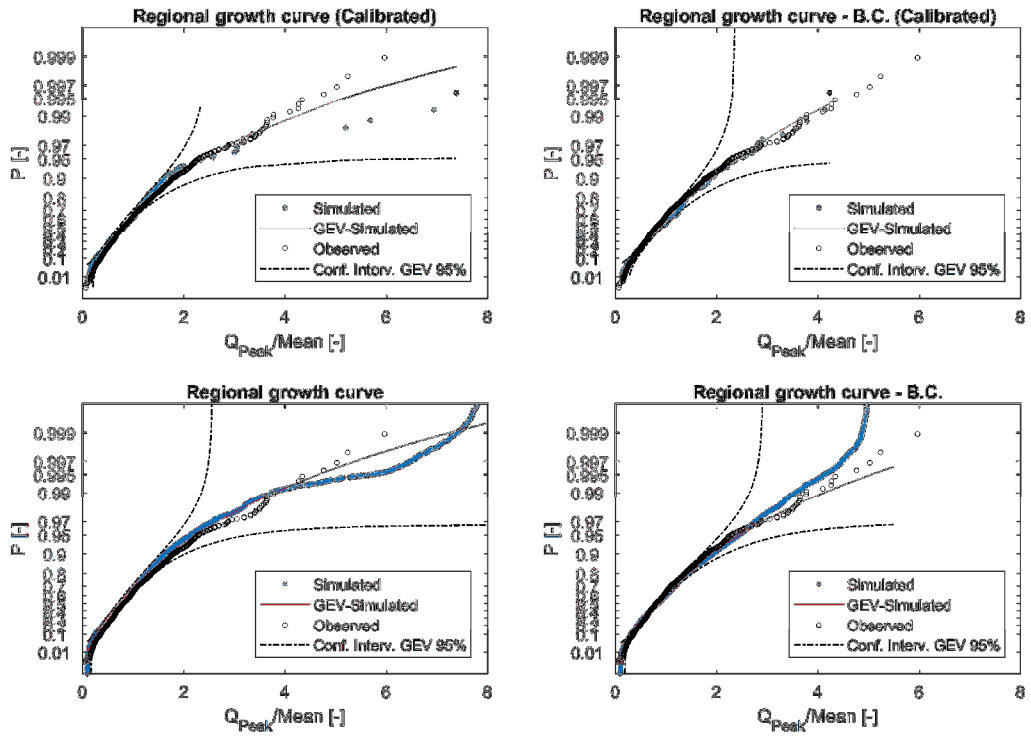
Figure 11. Sample growth curve obtained by model chain (blue dots) compared with observations (black dots). Red line is the GEV distribution fitted on modeled values while dotted lines are the confidence intervals with significance 95%. Top panels: results without and with rainfall bias correction using the sections where hydrological model was calibrated.

Bottom panels: results without and with rainfall bias correction using all the grid points with drainage area larger than A_{th}.
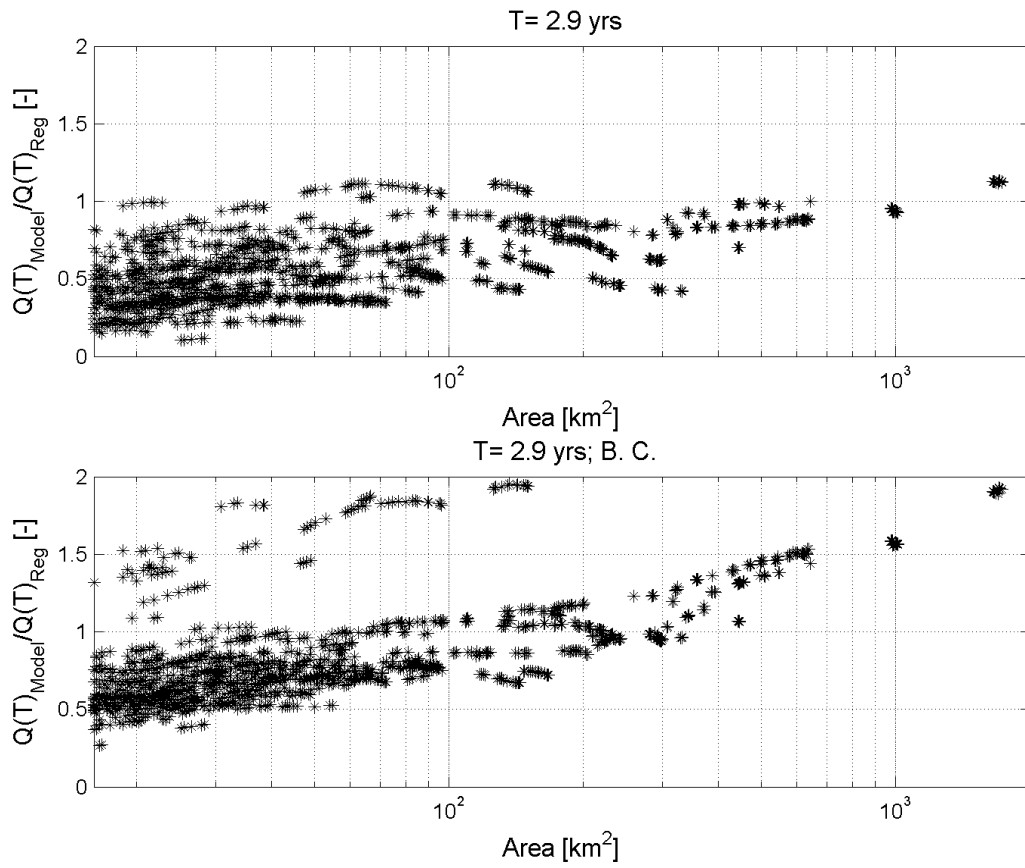
Figure 12. Ratio(T) as a function of drainage area. T=2.9 years which correspond to index flow. Upper panel shows results without rainfall bias correction, lower panel (B.C.) with rainfall bias correction.
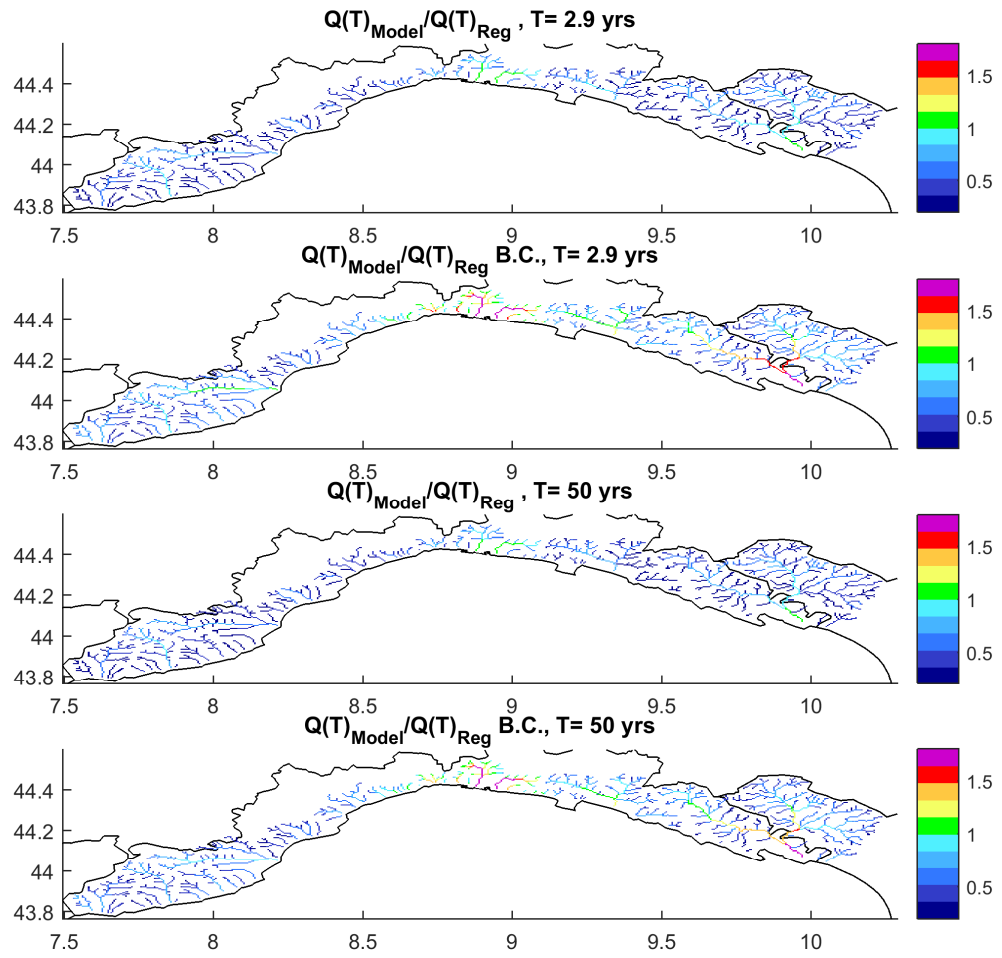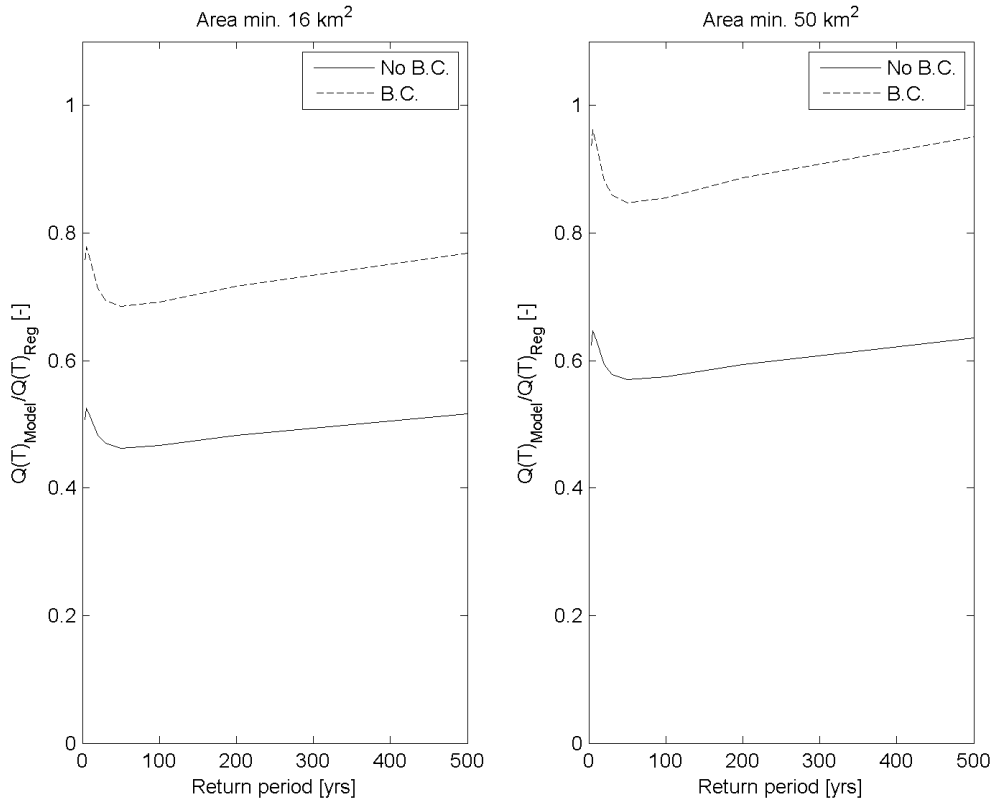
Figure 13. Maps of Ratio(T) for T=2.9 and 50 years. Upper panel shows results without rainfall bias correction, lower panel (B.C.) with rainfall bias correction. The B.C. increases the percentage of drainage network points that have values around 1.

1

Figure 14. Mean Ratio(T) over the considered domain as a function of T. Continuous line (no
B.C.) is the case without rainfall bias correction, dotted line (B.C.) is the case with rainfall
bias correction. Left panel is the case where points with drainage area lower than 16 km^2 are
discarded; right panel is the case where points with drainage area lower than 50 km^2 are
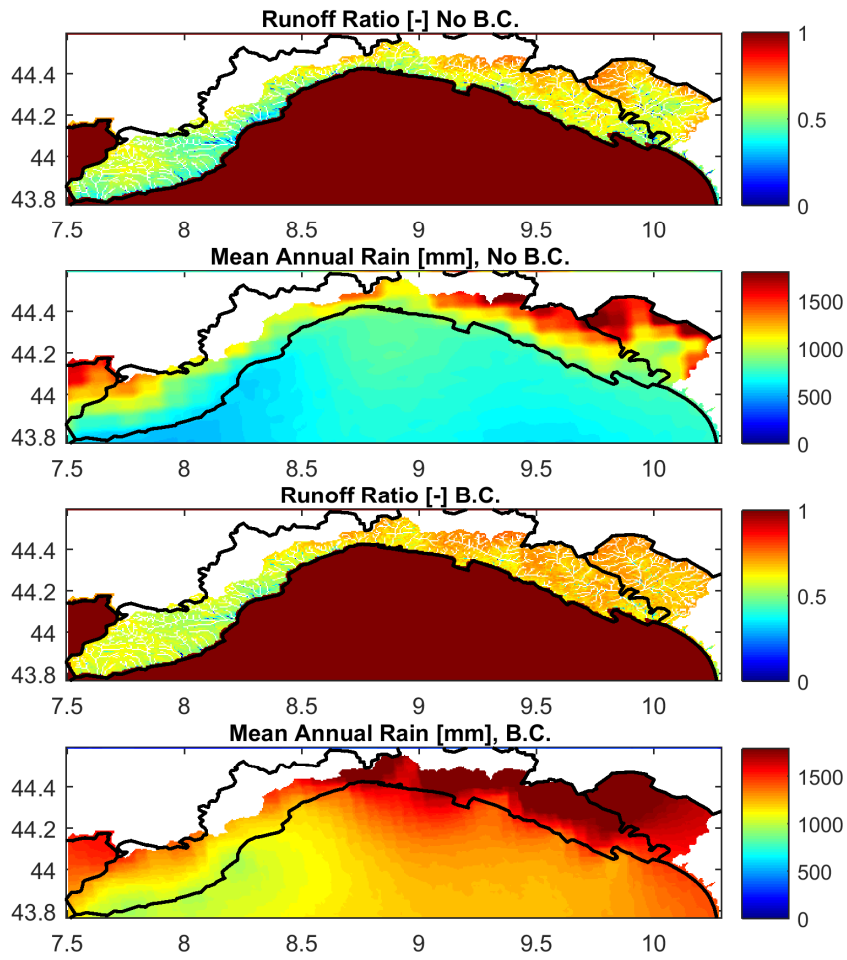discarded.

1
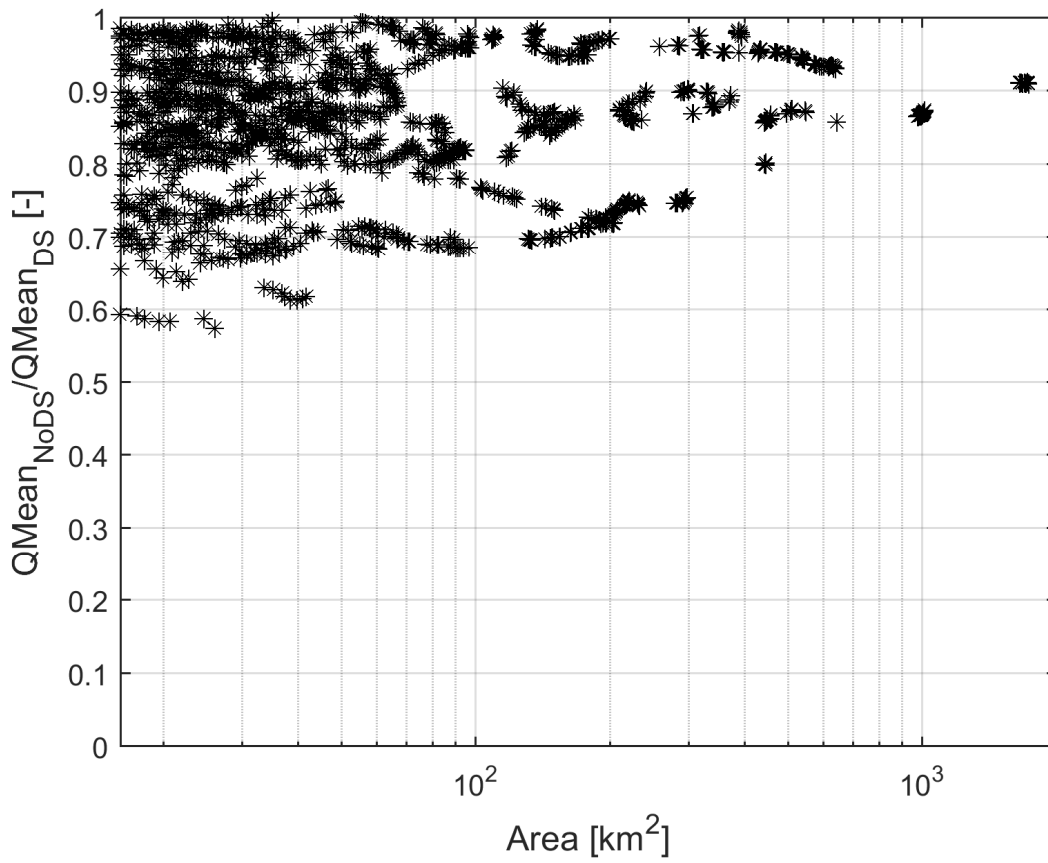
2

3 Figure 15. Ratio between mean flow estimated without and with downscaling as a function of

4 drainage Area. The graph shows that the impact of rainfall downscaling increases when basin

5 drainage area decreases.

6

7

1
2

3

4   Figure 16. Distributed runoff ratio and mean annual rainfall. Upper panels show the

5   model estimation without B.C. while lower panels with B.C. .

6